Gamma-Ray Bursts in the *Swift* Era

N. Gehrels,[1] E. Ramirez-Ruiz,[2] and D.B. Fox[3]

[1]NASA-Goddard Space Flight Center, Greenbelt, Maryland 20771; email: gehrels@milkyway.gsfc.nasa.gov

[2]Department of Astronomy and Astrophysics, University of California, Santa Cruz, California 95064; email: enrico@ucolick.org

[3]Department of Astronomy and Astrophysics, Pennsylvania State University, University Park, Pennsylvania 16802; email: dfox@astro.psu.edu

Annu. Rev. Astron. Astrophys. 2009. 47:567–617

The *Annual Review of Astronomy and Astrophysics* is online at astro.annualreviews.org

This article's doi:
10.1146/annurev.astro.46.060407.145147

0066-4146/09/0922-0567$20.00

Key Words

cosmology: early universe; galaxies: interstellar medium, high-redshift; gamma rays: observations, theory; stars: Wolf-Rayet, neutrinos; supernovae: general, gravitational waves

Abstract

With its rapid-response capability and multiwavelength complement of instruments, the *Swift* satellite has transformed our physical understanding of γ-ray bursts (GRBs). Providing high-quality observations of hundreds of bursts, and facilitating a wide range of follow-up observations within seconds of each event, *Swift* has revealed an unforeseen richness in observed burst properties, shed light on the nature of short-duration bursts, and helped realize the promise of GRBs as probes of the processes and environments of star formation out to the earliest cosmic epochs. These advances have opened new perspectives on the nature and properties of burst central engines, interactions with the burst environment from microparsec to gigaparsec scales, and the possibilities for nonphotonic signatures. Our understanding of these extreme cosmic sources has thus advanced substantially; yet, more than 40 years after their discovery, GRBs continue to present major challenges on both observational and theoretical fronts.

1. INTRODUCTION

1.1. Setting the Stage

Gamma-ray bursts (GRBs) are among the most fascinating phenomena in the Universe. They are bright flashes of radiation with spectral energy distributions peaking in the γ-ray band. They have durations measured in seconds and appear to be capable of producing directed flows of relativistic matter with kinetic luminosities exceeding 10^{53} erg s^{-1}, making them the most luminous events known. All evidence points to a gravitational power source associated with the cataclysmic formation of a relativistic star or to a precursor stage whose inevitable end point is a stellar-mass black hole (BH).

The field of GRB astronomy has been greatly stimulated by the launch of the *Swift* satellite (Gehrels et al. 2004) in 2004, with its rapid response and panchromatic suite of instruments onboard, and by the development of new-technology robotic telescopes on the ground. A multidisciplinary approach is now emerging, with data combined across the electromagnetic spectrum to learn about the physical processes at play; "spectral chauvinism" can no longer be tolerated in the modern study of GRBs. Even nonphotonic neutrino and gravitational-wave instruments are becoming more sensitive and may soon be detecting signatures related to GRBs.

Although interesting on their own, GRBs are now rapidly becoming powerful tools to study detailed properties of the galaxies in which they are embedded and of the Universe in general. Their apparent association with massive star formation and their brilliant luminosities make them unique probes of the high-redshift Universe and galaxy evolution. Absorption spectroscopy of GRB afterglows is being used to study the interstellar medium (ISM) in evolving galaxies, complementary to the traditional studies of quasar absorption line systems. Possibly the most interesting use of GRBs in cosmology is as probes of the early phases of star and galaxy formation, and the resulting reionization of the Universe at $z \sim 6$–20. GRBs are bright enough to be detectable, in principle, out to much larger distances than the most luminous quasars or galaxies detected at present. Thus, promptly localized GRBs could serve as beacons that, shining through the pregalactic gas, provide information about much earlier epochs in the history of the Universe.

Before the advent of *Swift*, the study of GRBs had evolved somewhat unsystematically. As a result, the field has a large number of historical curiosities such as complex classification schemes that are now becoming streamlined as the field matures. Objects once thought to be different are now found to be related, and the style of research has shifted from piecewise studies to a more general statistical approach. Although leaps in understanding can still come from extraordinary events, as we show in several examples in this review, the applications to broader astrophysics are coming from the compilations of hundreds of events. The literature on this subject has therefore become quite large, and we apologize for referring now and then only to the most recent comprehensive article on a given topic. Several recent summary articles give excellent reviews in specific areas related to GRBs. These include the supernova-burst connection (Woosley & Bloom 2006), short GRBs (Lee & Ramirez-Ruiz 2007, Nakar 2007a), afterglows (van Paradijs, Kouveliotou & Wijers 2000; Zhang 2007), and theory (Mészáros 2002). Our objective here is to summarize the field of GRB astronomy from the *Swift* era and prior to the next steps with the *Fermi Gamma Ray Observatory* (Atwood et al. 2009), interpreting past findings while looking ahead to future capabilities and potential breakthroughs.

1.2. A Burst of Progress

The first sighting of a GRB came on July 2, 1967, from the military *Vela* satellites monitoring for nuclear explosions in violation of the Nuclear Test Ban Treaty (Klebesadel, Strong & Olson

1973). These γ-ray flashes, fortunately, proved to be different from the man-made explosions that the satellites were designed to detect, and a new field of astrophysics was born. Over the next 30 years, hundreds of GRBs were detected. Frustratingly, they continued to vanish too soon to get an accurate angular position for follow-up observations. The reason for this is that γ-rays are notoriously hard to focus, so γ-ray images are generally not very sharp.

Before 1997, most of what we knew about GRBs was based on observations from the Burst and Transient Source Experiment (BATSE) on board the *Compton Gamma-Ray Observatory*, whose results were summarized by Preece et al. (2000). BATSE, which measured about 3000 events, revealed that between two and three visible bursts occur somewhere in the Universe on a typical day. While they are on, they can outshine every other source in the γ-ray sky, including the sun. Although each is unique, the bursts fall into one of two rough categories. Bursts that last less than two seconds are "short," and those that last longer—the majority—are "long." The two categories differ spectroscopically, with short bursts having relatively more high-energy γ-rays than long bursts do.

Arguably the most important result from BATSE concerned the distribution of bursts. They occur isotropically—that is, evenly over the entire sky—suggesting a cosmological distribution with no dipole and quadrupole components. This finding cast doubt on the prevailing wisdom, which held that bursts came from sources within the Milky Way. Unfortunately, γ-rays alone did not provide enough information to settle the question for sure. The detection of radiation from bursts at other wavelengths would turn out to be essential. Visible light, for example, could reveal the galaxies in which the bursts took place, allowing their distances to be measured. Attempts were made to detect these burst counterparts, but they proved fruitless.

A watershed event occurred in 1997, when the *BeppoSAX* satellite succeeded in obtaining high-resolution X-ray images (Piro et al. 1999) of the predicted fading afterglow of GRB970228—so named because it occurred on February 28, 1997. This detection, followed by a number of others at an approximate rate of 10 per year, led to positions accurate to about an arc minute, which allowed the detection and follow-up of the afterglows at optical and longer wavelengths ([e.g., van Paradijs et al. 1997; we note, however, that the first optical afterglow detection of GRB GRB970228 (van Paradijs et al. 1997) was based on the X-ray prompt detection by *BeppoSAX*.]. This paved the way for the measurement of redshift distances, the identification of candidate host galaxies, and the confirmation that they were at cosmological distances (Metzger et al. 1997).

Among the first GRBs pinpointed by *BeppoSAX* was GRB970508 (Metzger et al. 1997). Radio observations of its afterglow provided an essential clue. The glow varied erratically by roughly a factor of two during the first three weeks, after which it stabilized and then began to diminish (Frail et al. 1997). The large variations probably had nothing to do with the burst source itself; rather, they involved the propagation of the afterglow light through space. Just as the Earth's atmosphere causes visible starlight to twinkle, interstellar plasma causes radio waves to scintillate. Therefore, if GRB970508 was scintillating at radio wavelengths and then stopped, its source must have grown from a mere point to a discernible disk. "Discernible" here means a few light-weeks across. To reach this size, the source must have been expanding at a considerable rate—close to the speed of light (Waxman, Kulkarni & Frail 1998).

The observational basis for a connection between GRBs and supernovae was provided by the discovery that the *BeppoSAX* error box of GRB980425 contained supernova SN1998bw (Galama et al. 1998). A number of other GRBs have since shown a 1998bw-like temporal component superposed on the power-law optical light curve (Woosley & Bloom 2006), but they still lacked a clear spectroscopic detection of an underlying supernova. Detection of such a signature came with the discovery of GRB030329 by the *High Energy Transient Explorer* (*HETE-2*) (Stanek et al. 2003, Hjorth et al. 2003). Because of its extreme brightness and slow decay, spectroscopic observations

were extensive. The early spectra consisted of a power-law decay continuum ($F_\nu \propto \nu^{-0.9}$) typical of GRB afterglows with narrow emission features identifiable as Hα, [O III], Hβ, and [O II] at $z = 0.1687$ (Kawabata et al. 2003, Matheson et al. 2003), making GRB030329 the second-nearest burst overall at the time and the nearest classical burst. [The other GRBs with supernova associations have been underluminous events (Kaneko et al. 2007).] A major contribution to our understanding of X-ray prompt emission also came from the *HETE-2* mission (Lamb et al. 2004), which was active from 2000 to 2006. Dozens of bursts in the "X-ray flash" category were observed and were found to be similar in origin to the classical long GRBs (Matsuoka et al. 2004).

Swift is the current GRB discovery mission. It is a space robot designed specifically with GRBs in mind. It combines a wide-field hard X-ray burst detection telescope (Burst Alert Telescope—BAT; Barthelmy et al. 2005a) with narrow-field X-ray (X-Ray Telescope—XRT; Burrows et al. 2005a) and ultraviolet-optical (UV Optical Telescope–UVOT; Roming et al. 2005) telescopes. A powerful and fast onboard burst-detection algorithm (Fenimore et al. 2003) provides the burst coordinates to the spacecraft, which autonomously repoints the observatory so that X-ray and optical observations typically commence within two minutes of the burst trigger. The mission was designed to find counterparts for all burst types, including the previously elusive short GRBs. Burst positions and other data are provided promptly to ground observers.

The burst detection rate for *Swift* is ~100 GRBs per year, resulting in a current data set as of December 2008 of 380 bursts. Of these, there are 126 with redshift determination, mostly from spectrographs on large optical telescopes and new robotic telescopes on the ground. These now far outnumber the ~40 GRB redshifts available prior to *Swift*. More than 95% of the *Swift* bursts have X-ray afterglow detection and ~60% have optical afterglows (UVOT + ground). To date 33 short bursts have been localized with 8 having redshift determinations. The new data have enabled much more detailed studies of the burst environment, the host galaxy, and the intergalactic medium. *Swift* and follow-up observations have also transformed our view of GRB sources. For example, as discussed in Section 3, the old concept of a sudden release of energy concentrated in a few seconds has been discarded. Indeed, even the term "afterglow" is now recognized as misleading—the energy radiated during both phases is comparable.

Our primary intentions in this review are to describe the most important observational discoveries of the *Swift* era and to explain how the understanding of these events has been evolving, as a consequence. We hope to communicate these developments to an astronomical audience with little prior exposure to GRBs. Four sections follow. Section 2 describes our current knowledge of what constitutes a GRB. Section 3 summarizes the observations of the prompt and afterglow emission, and Section 4 summarizes observations of host galaxies and progenitor clues. In Section 5, we examine our current progress in understanding the basic physical processes at work. Section 6 is a look forward at future prospects for GRB study.

2. WHAT IS A γ-RAY BURST?

GRBs are sudden, intense flashes of γ-rays which, for a few blinding seconds, light up an otherwise fairly faint γ-ray sky. Spectra extending over many decades in photon energy have now been measured for hundreds of GRBs. In **Figure 1**, representative spectra are plotted in the conventional coordinates ν and νF_ν, the energy radiated per logarithmic (natural log) frequency interval. Some basic points should be emphasized. First, we measure directly only the energy radiated in the direction of the Earth per second per steradian per logarithmic frequency interval. The apparent bolometric luminosity may be quite different from the true bolometric luminosity if the source is not emitting isotropically. Second, there is striking evidence for a characteristic photon energy (peak in the νF_ν spectrum), which appears to be related to the overall spectral luminosity

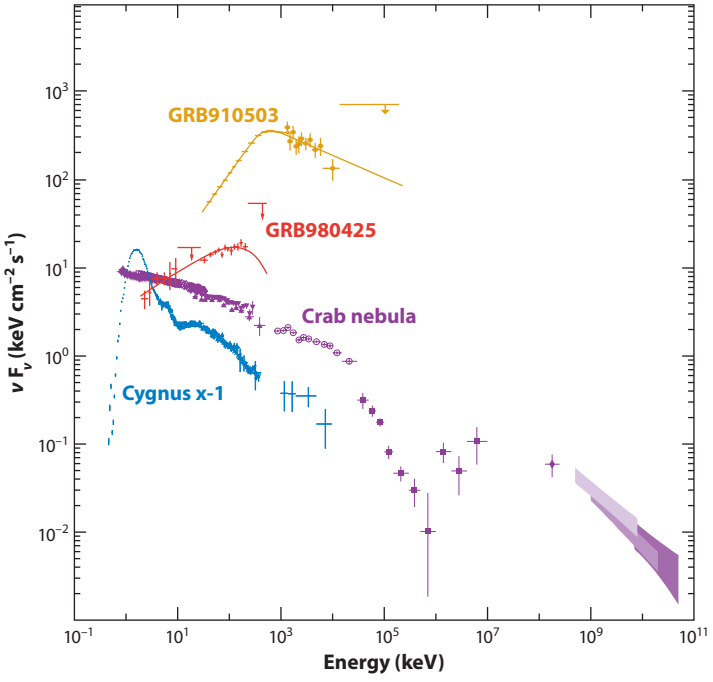

Figure 1

Gamma-rays are excellent probes of the most energetic phenomena in nature, which typically involve dynamical nonthermal processes and include interactions of high-energy electrons with matter, photons, and magnetic fields; high-energy nuclear interactions; matter–antimatter annihilation; and possibly other fundamental particle interactions. Shown here are representative spectra $\nu F_\nu \propto \nu^2 N(\nu)$ of γ-ray bursts (GRBs) (Kaneko et al. 2007, 2008) along with the Crab pulsar nebula (Kuiper et al. 2001) and the galactic black hole candidate Cygnus X-1 (McConnell et al. 2002).

normalization. In contrast, the spectra of many galactic and extragalactic accretion systems are often well fitted by single power-laws. A simple power-law contains little information, whereas a complex spectrum composed of many broken power-laws tells us much more, as each break frequency must be explained.

At cosmological distances, the observed GRB fluxes imply energies that can exceed 10^{53} $(\Omega/4\pi)$ erg, where Ω is the solid angle of the emitting region (**Figure 2**; see also Bloom, Frail & Sari 2001). This is the mass equivalent of 0.06 $M_\odot$ for the isotropic case. Compared with the size of the sun, the seat of this activity is extraordinarily compact, with sizes of less than milli-light-seconds (<300 km) as indicated by rapid variability of the radiation flux (Bhat et al. 1992). It is unlikely that mass can be converted into energy with better than a few (up to ten) percent efficiency; therefore, the more powerful GRB sources must "process" upwards of $10^{-1}(\Omega/4\pi)M_\odot$ through a region not much larger than a neutron star (NS) or a stellar-mass black hole (BH). No other entity can convert mass to energy with such high efficiency or within such a small volume.

The observed γ-rays have a nonthermal spectrum. Moreover, they commonly extend to energies above 1 MeV, the pair production threshold in the rest frame. These facts together imply that the emitting region must be relativistically expanding (Guilbert, Fabian & Rees 1983; Goodman 1986; Paczyński 1986). We draw this conclusion for two reasons. First, if the region were indeed only a light-second across or less, as would be implied by the observed rapid variability in the absence of relativistic effects, the total mass of baryons in the region would need to be below

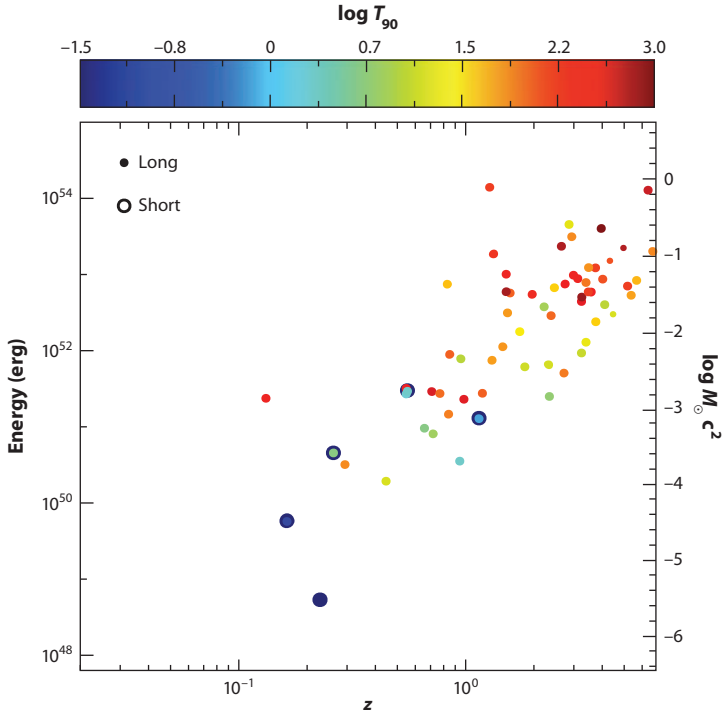

Figure 2

Apparent isotropic γ-ray energy as a function of redshift and observed duration. The energy is calculated assuming isotropic emission in a common comoving bandpass for a sample of short and long GRBs with measured redshifts. This spread in the inferred luminosities obtained under the assumption of isotropic emission may be reduced if most GRB outflows are jet-like. A beamed jet would alleviate the energy requirements, and some observational evidence does suggest the presence of a jet.

$\sim 10^{-12}\ M_\odot$ in order that the electrons associated with the baryons should not provide a large opacity (Piran & Shemi 1993, Paczyński 1990). Second, larger source dimensions are required in order to avoid opacity due to photon-photon collisions. If the emitting region is expanding relativistically, then, for a given observed variation time scale, the dimension R can be increased by Γ^2. The opacity to electrons and pairs is then reduced by Γ^4, and the threshold for pair production, in the observer frame, goes up by $\sim\Gamma$ from its rest-frame value (Fenimore et al. 1993; Woods & Loeb 1995; Baring & Harding 1997; Granot, Cohen-Tanugi & do Couto e Silva 2008). Best-guess numbers are Lorentz factors Γ in the range 10^2 to 10^3 (Lithwick & Sari 2001), allowing rapidly variable emission to occur at radii in the range 10^{12} to 10^{14} cm.

Because the emitting region must be several powers of ten larger than the compact object that acts as a trigger, there are further physical requirements. The original internal energy contained in the radiation and pairs would, after expansion, be transformed into relativistic kinetic energy. A variant that has also been suggested is based on the possibility that a fraction of the energy is carried by Poynting flux (Blandford & Znajek 1977, Usov 1992). This energy cannot be efficiently radiated as γ-rays unless it is rerandomized (Narayan, Paczyński & Piran 1992; Mészáros, Rees & Papathanassiou 1994; Paczyński & Xu 1994; Rees & Mészáros 1994). Impact on an external medium (or an intense external radiation field; see, e.g., Shaviv & Dar 1995) would randomize half of the initial energy merely by reducing the expansion Lorentz factor by a factor of two.

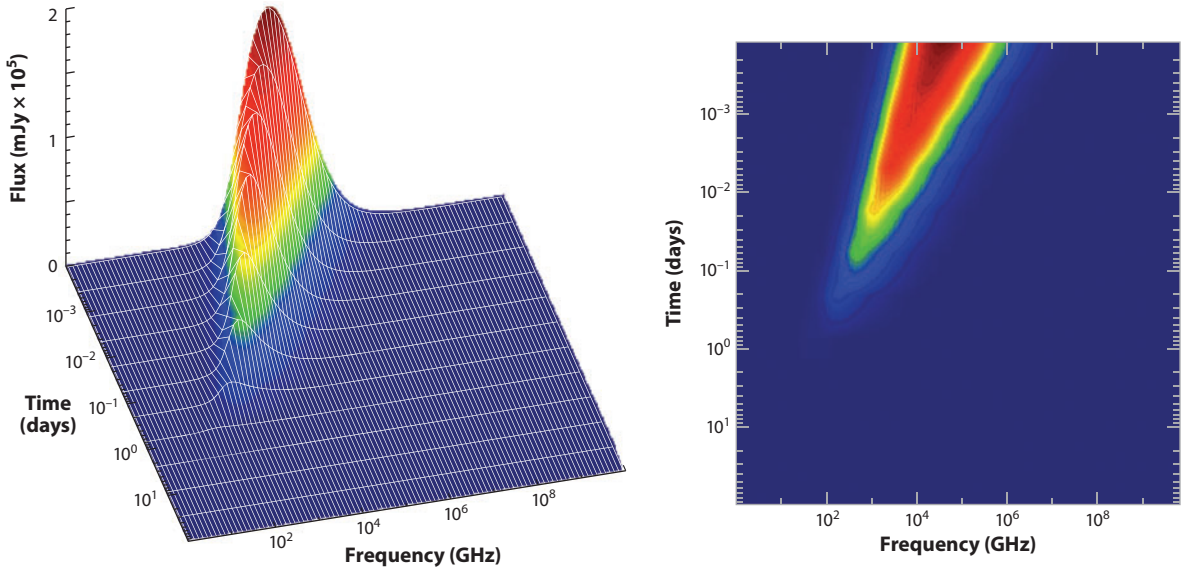

Figure 3

The evolving synchrotron afterglow of a γ-ray burst. Shown is a theoretical model (Gou, Fox & Mészáros 2007) for the afterglow of the *Swift* GRB050904. The model is presented without extinction and as it would have been observed at redshift $z = 2$; the burst itself occurred at $z = 6.29$. The evolution of the synchrotron peak to lower frequencies is clearly visible. More subtle effects, including evolution of the synchrotron cooling and self-absorption frequencies, and the associated synchrotron self-Compton emission of the blastwave at higher frequencies are not readily visible in this model.

For an approximately smooth distribution of external matter, the bulk Lorentz factor of the fireball thereafter decreases as an inverse power of the time. In the presence of turbulent magnetic fields built up behind the shocks (Rees & Mészáros 1992), the electrons produce a synchrotron power-law radiation spectrum that softens in time as the synchrotron peak corresponding to the minimum Lorentz factor and field decreases during the deceleration (Katz 1994; Sari, Narayan & Piran 1996). Thus, the GRB radiation, which started out concentrated in the γ-ray range during the burst, is expected to progressively evolve into an afterglow radiation that peaks in the X-rays, then UV, optical, IR, and radio (**Figure 3**). Detailed predictions (Mészáros & Rees 1997) of the afterglow properties, made in advance of the observations, agreed well with subsequent detections at these photon energies, followed up over periods of up to months. The detection of diffractive scintillation in the radio afterglow of GRB970508 provided the first determination of the source size and a direct confirmation of relativistic source expansion (Frail et al. 1997), which were further strengthened by the size measurement of the afterglow image of GRB030329 by radio interferometry with the Very Long Baseline Array (VLBA) (Taylor et al. 2004).

The complex time-structure of some bursts suggests that the central engine may remain active for up to 100 s (Ramirez-Ruiz & Fenimore 2000) or possibly longer (Falcone et al. 2007). However, at much later times all memory of the initial time-structure would be lost; essentially all that matters is how much energy and momentum have been injected and their distribution in angle and velocity. We can at present only infer the energy per solid angle, but there are reasons to suspect that bursts are far from isotropic. Due to relativistic beaming, an observer will receive most emission from those portions of a GRB blast wave that are within an angle $\sim 1/\Gamma$ of the direction to the observer. The afterglow is thus a signature of the geometry of the ejecta—at late stages, if the outflow is beamed, we expect a spherically symmetric assumption to be inadequate; the deviations from the

predictions of such a model would then tell us about the ejection in directions away from our line of sight (Rhoads 1999).

The appearance of achromatic breaks in the development of GRB afterglows has been interpreted as indicating that they are jet flows beamed toward us. Collimation factors of $\Omega_i/4\pi \lesssim 0.01$ (corresponding to half opening angles of $\lesssim 8$ degrees) have been derived from such steepening (Frail et al. 2001; Bloom, Frail & Kulkarni 2003). If GRB sources are beamed, then this reduces the energy per burst by two or three orders of magnitude at the expense of increasing their overall frequency.

Regarding the central engine trigger, a number of key questions remain. What are the progenitors? What is the nature of the triggering mechanism, the transport of the energy, and the time scales involved? Does the trigger involve a hyperaccreting compact object? If so, can we tell how it was formed? The presence of some GRBs (in the short-duration category) in old stellar populations rules out a source uniquely associated with recent star formation and, in particular, massive star origin for all bursts (Gehrels et al. 2005, Bloom et al. 2006). An understanding of the nature of these sources is thus inextricably linked to the "metabolic pathways" through which gravity, spin, and energy can combine to form collimated, ultrarelativistic outflows. These threads are few and fragile, and the tapestry is as yet a poor image of the real Universe. If we are to improve our picture-making, we must make more and stronger ties to physical theory. But in reconstructing the engine, we must be guided by our eyes and their extensions. The following sections provide a detailed summary of the observed properties of these ultraenergetic phenomena. These threads are woven together in Section 5.

3. BURST AND AFTERGLOW OBSERVATIONS

The most direct diagnostics of the conditions within GRBs come from the radiation observations, which we summarize in this section. We do not intend to a give a detailed review of individual events because there are now sufficiently many examples that we are likely to be led seriously astray if we test our theories against individual events. For this reason, we center our discussion on major trends, even in cases in which the generalizations we describe are based on data that do not yet have the statistical weight of a "complete" sample. It should be noted that there are inherent biases in the discovery of a GRB at a given redshift that are often difficult to quantify, such as complex trigger efficiencies and nondetections. Continued advances in the observations will surely yield unexpected revisions and additions in our understanding of the properties of GRBs.

3.1. Prompt High-Energy Emission

3.1.1. Taxonomy. The manifestations of GRB activity are extremely diverse. GRBs are observed throughout the electromagnetic spectrum, from GHz radio waves to GeV γ-rays, but until recently, they were known predominantly as bursts of γ-rays, largely devoid of any observable traces at any other wavelengths. Gamma-ray properties provide only one of several criteria for classifying GRB sources. Part of the problem is observational because it is not possible to obtain full spectral coverage in all objects and it is not easy to reconcile a classification based on host-galaxy properties with one based on the prompt γ-ray properties. The major impediment to serious taxonomy is more fundamental. GRBs are heterogeneous objects, especially in their directly observed properties. The success of a classification scheme, we believe, should be measured by the extent to which newly recognized properties distinguish subsets defined by differences in other properties. By this criterion, the taxonomy of GRBs has met with only mixed success. As new non-γ-ray selection techniques are introduced (e.g., the age of stellar populations in host galaxies or the presence of type

Ic supernova signatures), the class boundaries (e.g., short- and long-duration events) have blurred where the defined subclasses transcend traditional boundaries. However, many new properties do correlate with old ones. This is all the more remarkable in that the conventional diagnostics (e.g., burst duration) measure properties on scales several orders of magnitude larger than that which we believe to be characteristic of the engine.

3.1.2. Observed durations and redshifts. GRBs traditionally have been assigned to different classes based on their duration—usually defined by the time during which the middle 50% (T_{50}) or 90% (T_{90}) of the counts above background are measured. On the basis of this criterion, there are two classes of GRBs—short and long—separated by ∼2 s duration. The initial hints for the existence of such classes (Cline & Desai 1974, Mazets et al. 1981) were followed by stronger evidence from ISEE-3 and *Konus-WIND* data (Norris et al. 1984) and by definite proof using large statistics from BATSE (Kouveliotou et al. 1993). BATSE results also showed that short bursts have a harder spectrum than long bursts (Kouveliotou et al. 1993), although this contrast is less prominent in observations by *Konus-WIND*, *HETE-2*, and *Swift* (Sakamoto et al. 2006).

The duration and redshift distributions for *Swift* GRBs are shown in **Figure 4**. The blue histogram in the left panel represents observed durations; the orange histogram shows the durations corrected to the source frame $T_{90}/(1+z)$ for those bursts with redshift determinations. In the source frame, the typical long-burst duration is ∼20 s compared to ∼50 s in the observer frame. *Swift* has been detecting a lower fraction (∼10%) of short bursts than BATSE did (25%). This is because *Swift* observes in a softer energy band (15–150 keV) than BATSE does (50 keV–2 MeV) and because *Swift* requires a sky image of the event for burst detection and the image part of the trigger algorithm is less sensitive to short bursts owing to their lower fluences. **Figure 4*b*** shows the measured redshift distributions. The blue histogram is for *Swift* events; the grey one is for pre-*Swift* bursts. It is clear that *Swift* is currently detecting GRBs at a higher average redshift: $\langle z \rangle \sim 2.5$ for *Swift* bursts versus $\langle z \rangle \sim 1.2$ for pre-*Swift* events. The reason for this difference is the higher sensitivity of *Swift* compared to *BeppoSAX* and *HETE-2*.

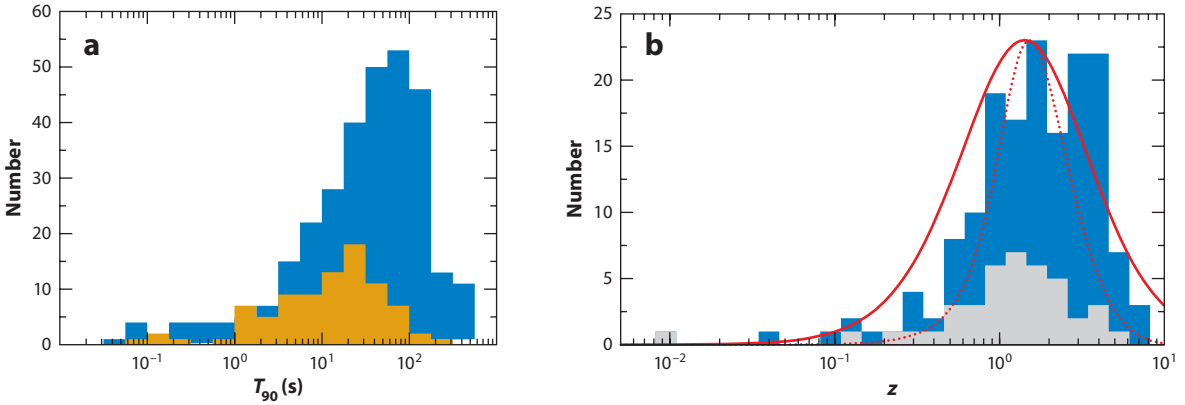

Figure 4

Duration and redshift distribution for *Swift* GRBs. (*a*) The duration distribution. The blue histogram is the measured T_{90} distribution; the orange one is corrected to the source frame: $T_{90}/(1+z)$. (*b*) The redshift distribution for *Swift* GRBs in blue and pre-*Swift* GRBs in grey. *Swift* is detecting higher redshift bursts on average than pre-*Swift*. The thick solid red theory curve illustrates the evolution of a comoving volume element of the Universe; the thin dotted red curve is a convolution of the comoving volume with a model for the star-formation rate as calculated by Porciani & Madau (2001).

GRBs have also been classified according to their spectral properties, albeit less successfully. In particular, bursts with lower spectral energy peaks (E_{peak}) have been denoted X-ray flashes (XRFs) based on observations by *BeppoSAX*, BATSE, and *HETE-2* (Heise et al. 2001, Barraud et al. 2003, Kippen et al. 2003, Sakamoto et al. 2005). These events are closely related to common long-duration GRBs and appear to form a continuum of all parameters between the two types with no striking evidence for a distinguishing characteristic (Granot, Ramirez-Ruiz & Perna 2005).

3.1.3. Observed correlations. There is a great deal of diversity in the γ-ray prompt light curves of GRBs. Both long and short bursts can have temporal profiles ranging from smooth, single-peaked pulses to highly structured multi-pulses. The prompt emission can be characterized by a variety of spectral and temporal parameters, which include duration, variability, lag, pulse rise/fall time, fluence, E_{iso}, and E_{peak}. A schematic diagram illustrating the most widely discussed γ-ray prompt correlations is shown in **Figure 5** with detailed references. These correlations are often based on statistical analysis of quantities whose physical causes are poorly understood but almost certainly depend on many variables. These correlations must therefore be interpreted with caution.

The prompt GRB light curves can generally be dissembled into a superposition of individual pulses as described by Norris et al. (1996), with rise times shorter on average than decay times (**Figure 5*f***). The variability or spikiness of the light curve is found to be correlated with peak luminosity or total isotropic energy of the burst (**Figure 5*a***). The time lag of individual peaks seen at different energy bands is observed to be anticorrelated with luminosity for long bursts (**Figure 5*b***). For short bursts, the lag is small or not measurable. The E_{peak} is also found to be correlated with E_{iso} for long bursts, including XRFs, with short bursts as clear outliers (**Figure 5*c***). The total isotropic energy emission is correlated with duration (**Figure 5*d***), with short and long bursts on approximately the same correlation line, albeit with a wide spread. Short bursts detected by *Swift* have lower E_{iso} on average than long bursts. There are three outliers belonging to the long-burst category, which are characterized by being significantly underluminous. These are GRBs 980425, 031203, and 060614.

Numerous researchers have studied ways to determine the absolute luminosity of a GRB using correlations such as those illustrated in **Figure 5**. These include the lag, variability, and E_{peak} correlations discussed above. Other interesting correlations have included E_{peak} versus E_γ (emitted energy corrected for beaming (Ghirlanda, Ghisellini & Lazzati 2004) and E_{peak} versus a duration-corrected peak luminosity (Firmani et al. 2006). The goal is to derive a method to determine the burst luminosity independently of a redshift distance determination, thus attempting to make GRBs standard candles that could be used, in principle, to determine the cosmic-expansion history of the Universe to higher redshift than is possible with supernovae. Although such efforts are currently under way (Schaefer 2006 and references therein), it is not clear at present whether any of these correlations are tight enough for significant progress to be made (Bloom, Frail & Kulkarni 2003).

3.1.4. Soft γ repeaters and short bursts. It has been noted (Hurley et al. 2005, Palmer et al. 2005, Nakar et al. 2006) that the giant flare (GF) observed from the putative galactic magnetar source SGR 1806-20 in December 2004 (Gaensler et al. 2005) could have looked like a typical short GRB had it occurred much farther away, thus making the telltale periodic signal characteristic of the NS rotation in the fading emission undetectable. The two previously recorded GFs of this type, one each from SGR 0520 – 66 on 5 March 1979 (Fenimore, Klebesadel & Laros 1996) and SGR 1900 + 14 on 27 August 1998 (Hurley et al. 1999), would have been detectable by existing instruments only out to ~8 Mpc, and it was therefore not previously thought that they could be the source of short GRBs. The main spike of the 27 December event would have resembled a

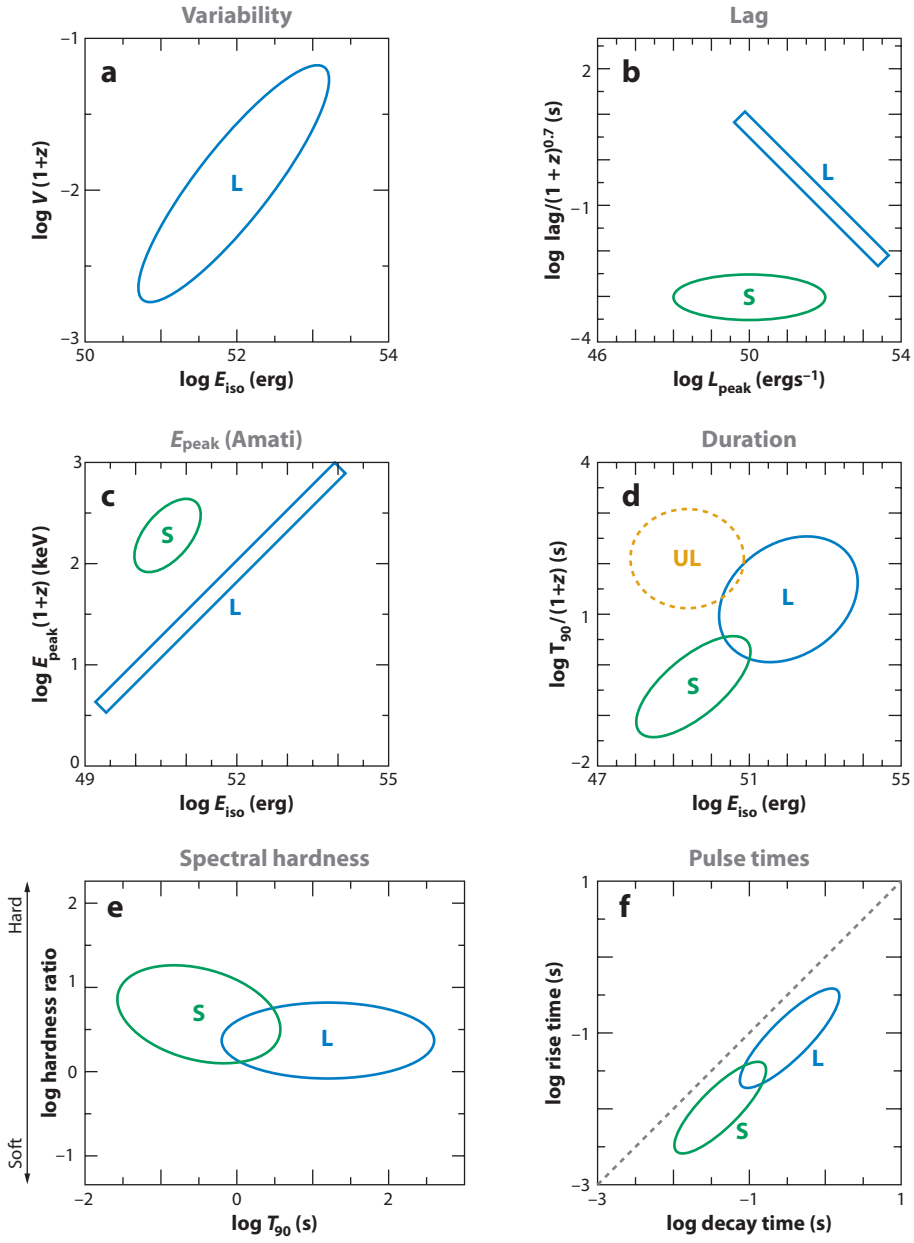

Figure 5

Schematic diagrams illustrating the most widely discussed correlations between various prompt emission properties for long (L), short (S), and underluminous (UL) GRBs. (*a*) Variability scaled to the burst frame versus E_{iso} (Fenimore & Ramirez-Ruiz 2000, Reichart et al. 2001, Schaefer 2006). The variability is a measure of the spikiness of the light curve and is defined as the mean square of the time signal after removing low frequencies by smoothing. (*b*) Spectral lag scaled to the burst frame versus peak luminosity (Norris & Bonnell 2006, Gehrels et al. 2006). (*c*) E_{peak} scaled to the burst frame versus E_{iso} (Amati et al. 2002 for *BeppoSAX* GRBs; Amati 2006 for *Swift* GRBs; Lloyd-Ronning & Ramirez-Ruiz 2002 for BATSE events). (*d*) Duration scaled to the burst frame versus E_{iso}. (*e*) Spectral hardness versus observed duration (Kouveliotou et al. 1993). (*f*) Pulse rise time versus its decay time (Norris et al. 1996).

short, hard GRB if it had occurred within ∼40 Mpc, a distance scale encompassing the Virgo cluster (Palmer et al. 2005). However, the paucity of observed GFs in our own Galaxy has so far precluded observationally based determinations of either their luminosity function or their rate. The observed isotropic distribution of short BATSE GRBs on the sky and the lack of excess events from the direction of the Virgo cluster suggest that only a small fraction, $\leq 5\%$, of these events can be SGR GFs within 40 Mpc (Palmer et al. 2005).

Before *Swift* detected short GRBs and their associated afterglow signatures, searches for nearby galaxies within narrow Interplanetary Network (IPN) error boxes revealed that only up to $\simeq 15\%$ of them could be accounted for by SGRs capable of producing GFs (Nakar et al. 2006). A recent, intriguing candidate is short GRB070201, which was observed by the IPN to have a location consistent with the arms of the nearby (0.8 Mpc) M31 galaxy (Mazets et al. 2008). A LIGO search for gravitational waves (Abbott et al. 2008) at the time of the burst turned up no signal, thereby excluding a compact merger origin. If the GRB was really in M31, it may have been an SGR GF. Although the fraction of SGR events among what are now classified as short GRBs may not be dominant, it should be detectable and can be tested with future *Swift* observations. It is also worth noting that some short GRBs likely originate in the local Universe (Tanvir et al. 2005).

3.2. Afterglow Observations

3.2.1. X-ray observations. *Swift* was designed to investigate the GRB afterglows by filling the temporal gap between observations of the prompt emission and the afterglow. The combined power of the Burst Alert Telescope (BAT) and X-Ray Telescope (XRT) has revealed that prompt X-ray emission smoothly transitions into the decaying afterglow (Barthelmy et al. 2005b, O'Brien et al. 2006). Three representative *Swift* X-ray light curves are shown in **Figure 6** for both long and short GRBs. These X-ray light curves start as early as 100 s after the GRB trigger and cover up to

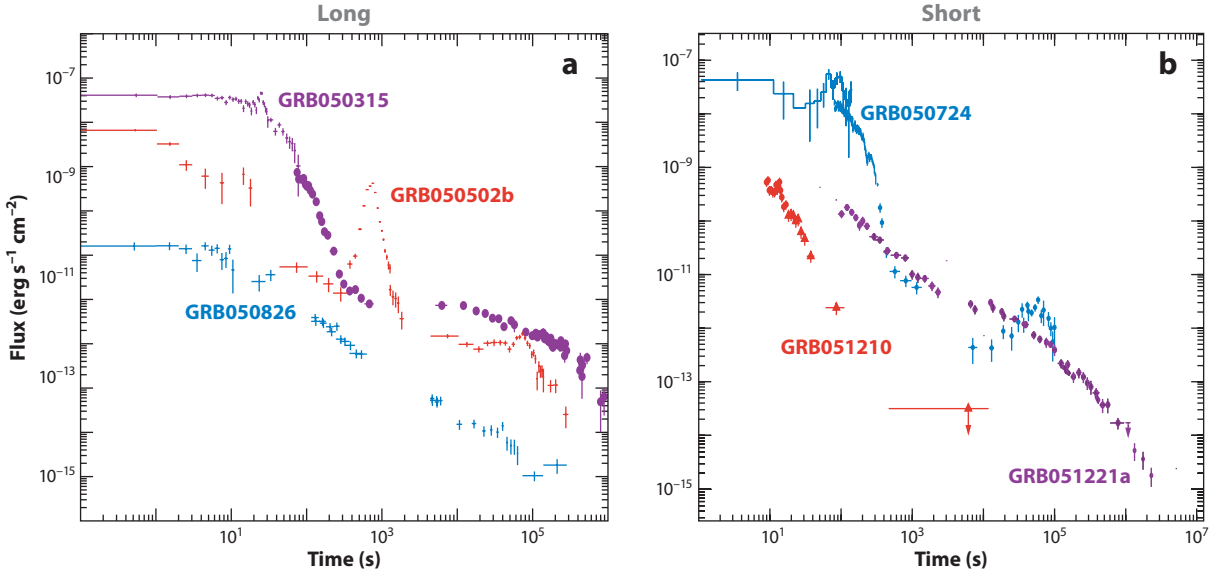

Figure 6

Representative examples of X-ray afterglows of (*a*) long and (*b*) short *Swift* events with steep-to-shallow transitions (GRB050315, 050724), large X-ray flares (GRB050502B, 050724), and rapidly declining (GRB051210) and gradually declining (GRB051221a, 050826; flux scale divided by 100 for clarity) afterglows.

Table 1 Typical parameters of the canonical *Swift* X-Ray Light Curve

Phase	Start T (s)	Decay index[a]	Approximate frequency
Steep decline	10^1–10^2	>3	50%
Shallow slope	10^2–10^3	0.5	60%
Classical afterglow	10^3–10^4	1.3	80%
Jet break late phase	10^5–10^6	2.3	20%[b]
X-ray flares	10^2–10^4		50%

[a]Decay index α defined by $F = F_0 t^{-\alpha}$.

[b]Of the 80% with no observed jet break, about half had afterglow observations terminate before expected time of jet break.

five decades in time. The complex behavior revealed in them significantly challenges traditional afterglow theory and calls into question some of the basic underlying assumptions.

One of the most striking results is that many of the early X-ray afterglows show a canonical behavior, where the light curve broadly consists of three distinct power-law segments (Nousek et al. 2006). A bright rapid-falling ($t^{-\alpha}$ where $\alpha > 3$) afterglow immediately after the prompt emission (Tagliaferri et al. 2005) is followed by a steep-to-shallow transition, which is usually accompanied by a change in the spectrum power-law index. This is consistent with an interpretation (Nousek et al. 2006, Zhang et al. 2006) in which the first break occurs when the slowly decaying emission from the forward shock becomes dominant over the steeply decaying tail emission of the prompt γ-rays as seen from large angles (Kumar & Panaitescu 2000). Because these two components arise from physically distinct regions, their spectrum would generally be different. The shallow phase then transitions to the classical afterglow phase with no clear evidence for a spectral change. In some cases a "jet break" is seen at late times. The intermediate shallow flux stage is commonly interpreted as being caused by the continuous energy injection into the external shock (Nousek et al. 2006, Zhang et al. 2006) although orientation and complex jet structures have been also discussed as viable alternatives. The energy in the afterglow at these late times is estimated to be comparable to or smaller than that in the prompt gamma-ray emission, even when correcting for radiative losses from the afterglow shock at early times, implying a high efficiency of the prompt emission. The presence of the shallow decay phase implies that most of the energy in the afterglow shock was either injected at late times after the prompt gamma-ray emission was over or was originally in slow material that would not have contributed to the prompt gamma-ray emission. This requires the prompt gamma-ray emission mechanism to be significantly more efficient than previous estimates. If a significant fraction of the radiated energy goes to photon energies above the observed range, the efficiency requirements of the prompt emission become even more severe.

The average times, slopes, and frequencies characterizing these three distinct X-ray afterglow components are listed in **Table 1**. Most *Swift* X-ray light curves are broadly consistent with this basic temporal description, although in most cases we do not see all three power-law segments, either because not all are present or because of limited temporal coverage. The large variety of behaviors exhibited by afterglows at different times in their evolution can be seen in **Figure 7**, which shows the temporal history for each individual afterglow as well as the evolution of the cumulative X-ray afterglows luminosity for a large sample of *Swift* events with known redshift. Although broadly compatible with relativistic fireball models (Nousek et al. 2006, Zhang et al. 2006), the complex afterglow behavior that has been revealed poses new challenges of interpretation. The reader is referred to Granot (2008) for a more detailed account of the major strengths and weaknesses of the standard afterglow model, as well as some of the challenges that it faces in explaining recent

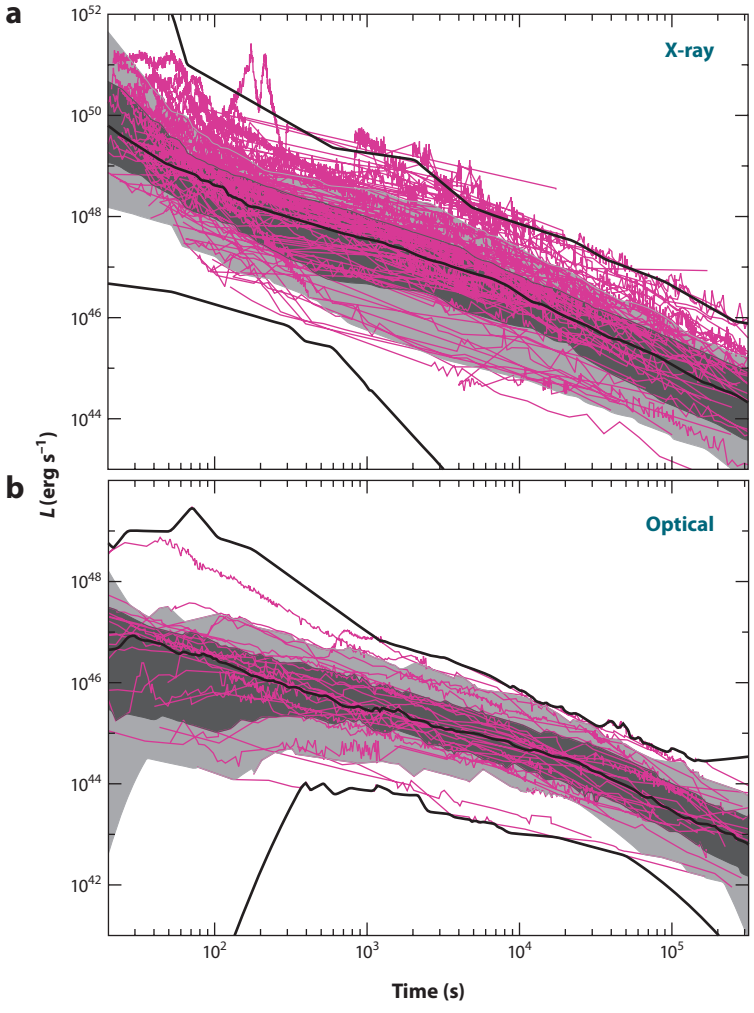

Figure 7

X-ray and optical light curves of GRB afterglows in the *Swift* era. (*a*) X-ray light curves of *Swift* burst afterglows. Data for long-duration bursts with known redshifts, from GRB050126 to GRB070724A, have been gathered from the *Swift* XRT light-curve and spectral data depository at the UK *Swift* Science Data Center (Evans et al. 2007, 2009). They are corrected uniformly to unabsorbed luminosity over 1.0–30.0 keV in the burst rest-frame, using the time-average afterglow spectrum, and plotted as a function of rest-frame time (*magenta lines*). Separately, afterglow light-curve fits (Racusin et al. 2009), which exclude flaring intervals, are used to construct minimum and maximum envelopes (*black lines*) and confidence intervals (*grey bands*) on the X-ray luminosities of the bursts as a function of rest-frame time: Light grey regions delimit bands of 10% to 90% confidence, dark grey regions delimit bands of 25% to 75% confidence, and the median burst luminosity at any given time is shown by the middle black line. (*b*) Optical light curves of *Swift* burst afterglows. Data for long-duration bursts with known redshifts and at least "bronze" quality published optical data (Kann et al. 2007), from GRB050408 to GRB070612A, are corrected uniformly to rest-frame U-band luminosity using the inferred R-band ($z = 1$) light curves from Kann et al. (2007) and plotted as a function of rest-frame time (*magenta lines*). Interpolated and "best fit" extrapolated light curves are used to generate minimum and maximum envelopes and median luminosity estimates (*black lines*) and confidence intervals (*grey regions*), as in *a*.

data. *Swift* has also discovered flaring behavior appearing well after the prompt phase in ∼50% of X-ray afterglows (Chincarini et al. 2007, Falcone et al. 2007). An illustration of bursts with bright flares is shown in **Figure 6**. In some extreme cases, the late-time flares have integrated energy similar to or exceeding the initial burst of γ-rays (Burrows et al. 2005b). The rapid rise and decay, multiple flares in the same burst, and cases of fluence comparable to the prompt emission suggest that these flares are due to the same mechanism responsible for the prompt emission, which is usually attributed to the activity of the central engine. When X-ray flares are observed by XRT, it is typically the case that no flaring is seen in the optical band by the UV Optical Telescope (UVOT). A notable example is GRB060418 (Molinari et al. 2007), whose optical-IR afterglow spectra are not consistent with a simple power-law extrapolation to soft X-ray energies and clearly requires two distinct spectral components. Not surprisingly, the broadband energy spectra of GRBs are complex and have wildly disparate shapes even though they belong to a single class.

Prior to *Swift*, there were several reports of emission and absorption line detections in the X-ray spectra of GRB afterglows. These included *BeppoSAX* observations of GRB970508 (Piro et al. 1999) and GRB000214 (Antonelli et al. 2000), ASCA observations of GRB970828 (Yoshida et al. 1999), *Chandra* observations of GRB991216 (Piro et al. 2000), and *XMM-Newton* observations of GRB011211 (Reeves et al. 2002). None of the detections were of high statistical significance, but, combined, were of some credibility. *Swift* has not found any significant line features in comprehensive observations of the X-ray afterglow of >200 GRBs (Romano et al. 2008). Hurkett et al. (2008) also made a very detailed *Swift* X-ray line search, with no positive result. These strong negative findings call into question the significance of previous results (see also Sako, Harrison & Rutledge 2005).

A final, widely discussed observational development is the discovery in ∼25% of short bursts detected by *Swift*/BAT of an extended emission (EE) component lasting for ∼100 s (Norris & Gehrels 2008). This component was clearly detected in *HETE-2* burst GRB050709 (Villasenor et al. 2005) and *Swift* burst GRB050724 (Barthelmy et al. 2005c). Archival searches have also found BATSE bursts with EE (Lazzati, Ramirez-Ruiz & Ghisellini 2001, Connaughton 2002, Norris & Bonnell 2006). The EE is typically softer than the main peak and has an intensity range from 10^{-3} to 10^{-1} times that of the initial short pulse complex. It is possible that many of the 75% of bursts without currently detected EE have this component at flux levels below detectability, although there are bursts with upper limits on the intensity of $<10^{-4}$ times that of the short pulse complex.

3.2.2. Optical observations. With increasing frequency during the *Swift* era, optical observations of GRBs have been commencing almost immediately after—and in one noteworthy case (GRB080319B; Racusin et al. 2008), prior to—the GRB trigger itself. These early optical observations have substantially enriched our appreciation for the complexity of the physical processes active during the prompt emission phase of GRBs and during the afterglow that follows. The large diversity of optical afterglow light curves can be seen in **Figure 7**.

3.2.2.1. Prompt Emission. Observations prior to the *Swift* era demonstrated already that bright optical flashes, such as that seen from GRB990123 (Akerlof et al. 1999), were relatively rare (Kehoe et al. 2001). The success of the *Swift* mission has brought a vast increase in the rate of bursts accessible to rapid optical follow-up and a corresponding increase in the number of events detected from early times, $t < 100$ s. The *Swift* UVOT itself routinely detects optical afterglows following the intial prompt slew of the satellite, with a 40% detection rate for such bursts (Roming et al. 2009) that is only slightly lower than the 60% detection rate of all observatories combined.

The fastest routine responses to *Swift* alerts are realized by robotic ground-based telescopes. The first discovery yielded by these observatories in the *Swift* era was of the γ-ray correlated

component of the prompt optical emission (Vestrand et al. 2005, 2006; Blake et al. 2005). This component is not observed in every burst, but the mere fact of its correlation is sufficient to establish a common origin with the prompt γ-ray emission (e.g., internal shocks). When observed, the ratio of the correlated γ-ray to optical flux densities has been found to be roughly 10^5 to 1.

In contrast to bursts with γ-ray correlated emission, the common burst is now revealed either to exhibit a single power-law decay from early times (Rykoff et al. 2005, Quimby et al. 2006, Yost et al. 2006) or to exhibit a flat or rising (Rykoff et al. 2004, 2006) or rebrightening (Stanek et al. 2007) optical light curve before it enters the standard power-law afterglow decay. The initial brightness of the typical counterpart is $V \sim 14$ to 17 mag (Roming et al. 2009), which has made observations challenging for smaller (<1 m) robotic facilities and has limited the extent of the light curves collected by the UVOT.

A few new observations of bright flaring optical emission have been collected, which are usually interpreted as emission from the reverse shock region (Sari & Piran 1999, Mészáros & Rees 1999). The early optical/near-IR emission from GRB041219 would have rivaled that seen from GRB990123 if not for the large galactic extinction along the line of sight (Vestrand et al. 2005). Of the three distinct peaks observed by PAIRITEL, the second may represent the onset of the afterglow (reverse shock) contribution (Blake et al. 2005); if so, a relatively small Lorentz factor, $\Gamma \sim 70$, is derived by associating the flaring peak time with the deceleration time of the relativistic blast wave. Observations of GRB050525A with UVOT (Blustin et al. 2006) and GRB060111B with TAROT (in a unique time-resolved tracking mode; Klotz et al. 2006) show the "flattening" light curve familiar from GRB021211 (Zhang, Kobayashi & Mészáros 2003). Intriguingly, the "high redshift" GRB050904 (Tagliaferri et al. 2005, Cusumano et al. 2006) at $z = 6.29$ (Kawai et al. 2006) also had prompt optical emission (Boër et al. 2006, Haislip et al. 2006), with a brightness, single-pulse structure, and fast-fading behavior reminiscent of GRB990123 and thus potentially also interpreted as reverse shock emission.

Swift detection of the "naked eye burst" GRB080319B, which peaked at visual magnitude $V = 5.3$, has now delivered the richest dataset, by far, addressing the prompt optical emission and its evolution into a standard fading afterglow (Racusin et al. 2008, Bloom et al. 2009, Woźniak et al. 2009). This is only partially due to the extreme brightness of the event; the fact that it occurred at an equatorial location, in the night sky above the Western hemisphere, is probably even more important. The fact that it occurred within just one hour and ten degrees of the preceding GRB080319A means that it is also the only event with strong constraints on optical precursor emission from pointed telescopes (Racusin et al. 2008). The GRB080319B dataset is rich enough that its ramifications are still being grappled with. In an overall sense, the prompt optical emission correlates well with the γ-ray light curve; in detail, though, the individual pulses observed in both bands do not track precisely, probably suggesting the presence of at least two distinct cooling processes at play within the dissipation region (Racusin et al. 2008). GRB080319B also allowed astronomers to rule out inverse Comptonization as a relevant mechanism (Piran, Sari & Zou 2009; Zou, Piran & Sari 2009).

3.2.2.2. Afterglow Emission. The observed properties of the optical afterglow are largely familiar from observations prior to the *Swift* era (van Paradijs, Kouveliotou & Wijers 2000; Mészáros 2002) and are not reviewed in detail here. An intriguing feature of later-time afterglows, revealed by the rich multiband light curves available in the *Swift* era, has been the occasional presence of chromatic light-curve breaks, where the X-rays show a clear break (steepening of the flux decay rate) whereas the optical does not. The break in the X-ray light curve is usually identified with the end of the shallow decay phase. The optical light curve follows a single power-law decay, usually with a temporal decay index intermediate between those in the X-rays before and after the break.

Accommodating such chromatic breaks in a model where the X-ray and optical emissions arise from the same emitting region (Panaitescu et al. 2006) requires not only a temporal evolution of the underlying microphysical conditions within the emitting region but also fine tuning their photon arrival times in such a way that a break in the X-ray will be produced but not at optical wavelengths. Alternatively, the X-ray and optical photons may arise from physically distinct regions, which would naturally account for their seemingly decoupled behavior. Observations of the naked-eye GRB080319B have sharpened this debate. This is because the optical and X-ray decays in this event exhibit discrepant behavior over two orders of magnitude in time, from 100 s to a few times 10^4 s postburst (Kumar & Panaitescu 2008, Racusin et al. 2008).

Recent results showed that during the initial 500 s of observations, 15% of UVOT light curves are seen to rise—with an average peak time of 400 s, 58% decay from the onset of observations, and the remainder are consistent with being flat, but could be rising or decaying (Oates et al. 2009). This leads to a wide range of temporal indices measured before 500 s, $-1.17 < \alpha < 0.21$. Such behavior is also observed by ground-based telescopes (Rykoff et al. 2005, 2006; Quimby et al. 2006; Yost et al. 2006) and was seen in pre-*Swift* observations (Rykoff et al. 2004). No color evolution was observed during the rising phase of the UVOT light curves. One likely scenario is that the rise is caused by the jet plowing into the external medium—the start of the forward shock. If this scenario is correct, then it is possible to determine the Lorentz factor of the jet at the time of the peak, giving Gamma ~180 and a lower limit Gamma >230 for those without observed peaks (Oates et al. 2009).

After a few hundred seconds, the afterglow decays as a single power-law with a temporal index, measured after 500 s, of $-1.20 < \alpha < -0.52$. This is consistent with pre-*Swift* observations, and the range is similar to the shallow decay of the XRT canonical model. However, 20% of UVOT light curves are seen with a broken power-law decay after 500 s. For these afterglows, the first decay has a range between $-0.74 < \alpha < -0.46$, which is most consistent with the shallow decay of the X-ray canonical light curve, and the second decay has a temporal range of $-1.72 < \alpha < -1.34$, which is most consistent with the classic afterglow phase.

At late times, $t \gtrsim 1$ day, it was common in the pre-*Swift* era to observe a steepening of the optical decay to power-law indices $\alpha_o > 2$, and to associate this epoch with the "jet break" transition of the underlying, relativistically expanding jet. As jet breaks are intrinsically achromatic, they are expected to manifest in the X-ray light curves from *Swift* as well as in ground-based optical observations. In fact, over the first three years of *Swift* operations, only a handful of convincing jet-break candidates were identified (Blustin et al. 2006, Stanek et al. 2007, Dai et al. 2007, Willingale et al. 2007, Kocevski & Butler 2008), leading to concerns about the viability of this picture. Some bursts with very long coverage have been convincingly shown to possess no significant breaks, e.g., GRB060729 (Grupe at al. 2007).

Since then, however, deep optical imaging observations have revealed evidence for jet breaks in several additional *Swift* afterglows, a significant fraction of those monitored to late times (Dai et al. 2008). Systematic analysis of the *Swift* XRT data has revealed strong evidence for a jet-break signature in 12% of the X-ray light curves (Racusin et al. 2009). A consensus has developed that jet breaks for typical *Swift* bursts may be occurring at late times and faint flux levels that are beyond the limit of the standard ground- and space-based campaigns. Separately, it has been suggested that a distinct additional spectral component could hide the jet-break signature in the X-ray band. For example, in the case of the bright GRB070125 (Chandra et al. 2008), inverse Compton scattering of the synchrotron optical photons has been put forward as an explanation for the missing jet-break feature.

3.2.3. Radio observations. Radio afterglow observations are unique in having led to both indirect and direct demonstrations of relativistic expansion, via scintillation (e.g., Chandra et al. 2008) and

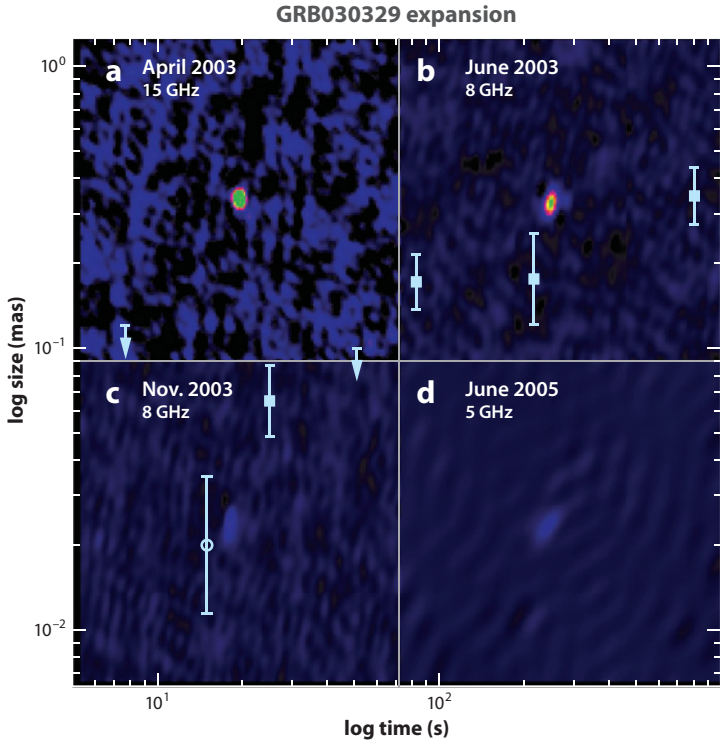

Figure 8

The growth of GRB030329 with time as measured using VLBI (Pihlström et al. 2007 and references therein). In the background are the images from (*a*) April 2003 (15 GHz), (*b*) June 2003 (8 GHz), (*c*) November 2003 (8 GHz), and (*d*) June 2005 (5 GHz) with the same intensity scale. The resolution for the four images is not constant in time, but this is accounted for in the analysis of the source size.

VLBI (very long baseline interferometry; Taylor et al. 2005) observations. They provide access to the properties of bright afterglows on the smallest angular scales. The limited number of sensitive high-resolution radio facilities and the sensitivity limits of those facilities have prevented a proportional exploitation of the greatly increased burst rate from *Swift*, primarily because the compensating feature of this increased burst rate has been a greater median redshift and a lower characteristic afterglow flux.

Radio afterglow observations nonetheless continue to play a vital role in accurately estimating blastwave kinetic energies (Oren, Nakar & Piran 2004; Granot, Ramirez-Ruiz & Loeb 2005; Kaneko et al. 2007). Radio detections have contributed crucially to the demonstration of the extremely large ($E \sim 10^{52}$ erg) kinetic energy associated with the high-redshift GRB050904 (Frail et al. 2006; Gou, Fox & Mészáros 2007) and to constraining the relativistic energy associated with the nearby GRB060218/SN2006aj (Soderberg et al. 2006b). Radio data can also provide a crucial "third check" on claims of jet-break detections, as with the broadband afterglow models applied to GRB050820 (Cenko et al. 2006) and GRB070125 (Chandra et al. 2008). For relatively nearby GRBs that may be associated with a supernova, radio observations have proven invaluable in providing evidence of the physical expansion of GRB/supernovae ejecta through direct imaging. **Figure 8** shows the expansion from ∼0.02 mas to ∼0.35 mas of the radio image of GRB030329 over a time span from ∼15 s after the GRB trigger to $\sim 10^3$ s (Pihlström et al. 2007).

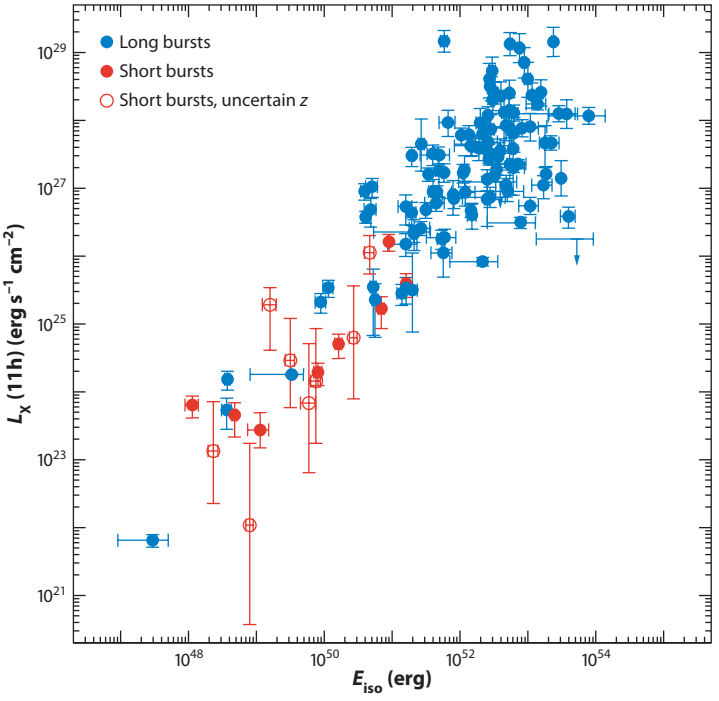

Figure 9

Isotropic-equivalent luminosity of GRB X-ray afterglows scaled to $t = 11$ h (5-keV source frame) after the burst trigger as a function of their isotropic γ-ray energy release (adapted from Nysewander, Fruchter & Pe'er 2009).

3.3. Interpreting Prompt and Afterglow Emission

The isotropic-equivalent luminosity of GRB X-ray afterglows scaled to $t \sim 11$ h after the burst in the source frame can be used as an approximate estimator for the energy in the afterglow shock for the following reasons (Freedman & Waxman 2001, Piran et al. 2001, Gehrels et al. 2008). First, at 11 h the X-ray band is typically above the two characteristic synchrotron frequencies, so that the flux has very weak dependence on microphysical parameters and no dependence on the external density, both of which are relatively poorly constrained. Second, at 11 h the Lorentz factor of the afterglow shock is sufficiently small ($\Gamma \sim 10$) so that a large fraction of the jet is visible (out to an angle of $\sim\Gamma^{-1} \sim 0.1$ rad around the line of sight) and local inhomogeneities on small angular scales are averaged out. Finally, the fact that the ratio of L_X (11 h) and $E_{\rm iso}$ is fairly constant for most GRBs suggests that both can serve as a reasonable measure of the isotropic-equivalent energy content of the ejected outflow.

Figure 9 shows L_X (11 h) at 5 keV rest-frame energy as a function of their isotropic γ-ray energy release for a large sample of GRBs. A linear relation, $L_X \propto (11\,{\rm h}) \propto E_{\gamma,{\rm iso}}$, seems to be broadly consistent with the data, probably suggesting a roughly universal efficiency for converting kinetic energy into γ-rays in the prompt emission for both long and short GRBs (Lee, Ramirez-Ruiz & Granot 2005; Nousek et al. 2006; Bloom et al. 2007; Kaneko et al. 2007; Nysewander, Fruchter & Pe'er 2009). This "universal" efficiency is also likely to be high (i.e., the remaining kinetic energy is comparable to, or even smaller than, the energy dissipated and radiated in the prompt emission). If this is the case, the well-known efficiency problem for long GRBs also persists for short events.

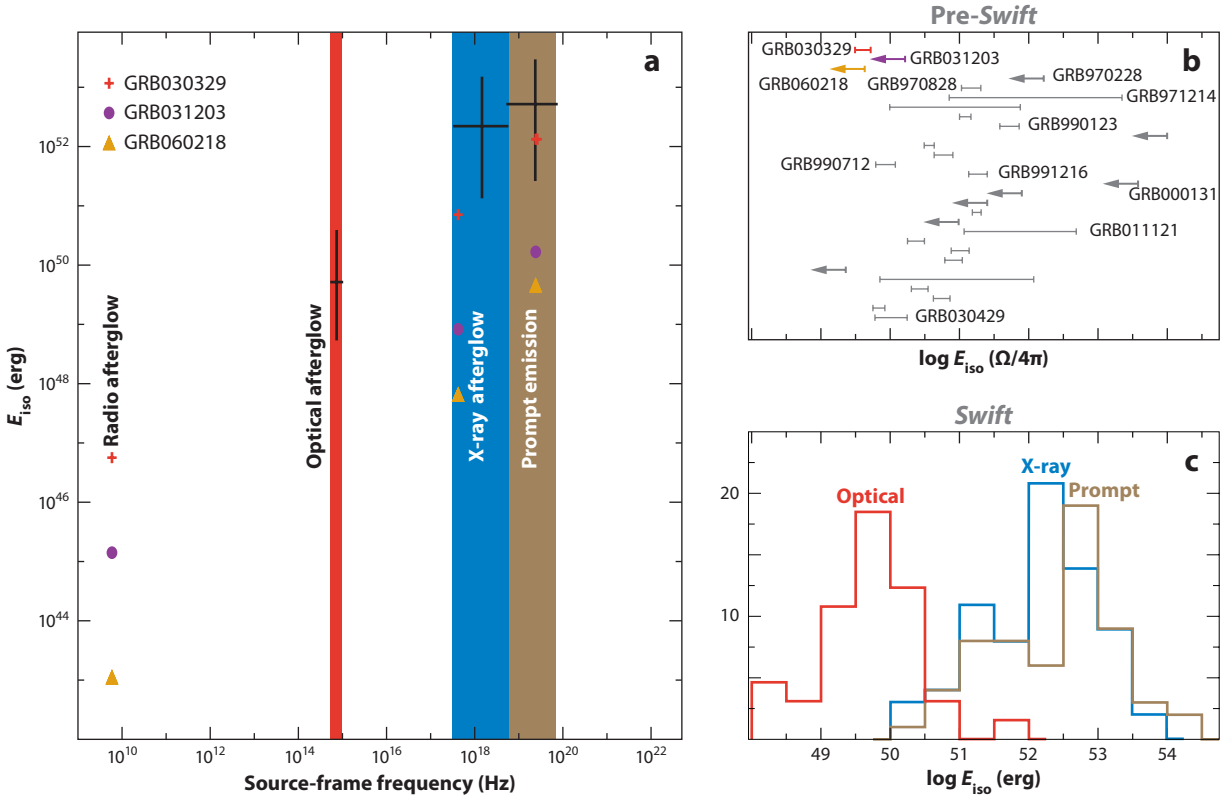

Figure 10

The radiated-energy inventory of *Swift* GRBs. (*a*) Summary of the isotropic-equivalent total emitted energy of the prompt and afterglow emission for *Swift* GRBs in the source frame (adapted from Kaneko et al. 2007). (*b*) Comparisons of collimation-corrected total emitted γ-ray energy, $E_{iso}(\Omega/4\pi)$, of pre-*Swift* GRBs, where E_{iso} is used as an upper limit for GRBs with no jet angle constraints. (*c*) Distributions of cumulative isotropic-equivalent total emitted energy for *Swift* GRBs.

3.4. The Radiated Energy Inventory

With the advent of *Swift*, the observational inventory for GRBs has become rich enough to allow estimates of their radiated energy content. A compilation of the radiated energy in both the prompt and afterglow phases is presented in **Figure 10**. To investigate the energy dissipation behavior in the X-ray and optical afterglow, we fitted a natural cubic spline function to the afterglow histories (shown in **Figure 7**) for each individual afterglow and estimated the cumulative emitted energy. The start and end times of the integration were the first and the last points of the actual observations. The result is a global portrait of the effects of the physical processes responsible for GRB evolution, operating on scales ranging from AU to parsec lengths. The compilation also offers a way to assess how well we understand the physics of GRBs.

Figure 10 shows that the isotropic X-ray emission, $E_{X,iso}$, for most *Swift* GRBs spans the range of $\sim 10^{50}$ to 10^{54} erg, which is comparable to that emitted during the prompt γ-ray phase. Not surprisingly, events that have large isotropic-equivalent energy in γ-rays have larger $E_{X,iso}$, indicating a reasonably narrow spread in the efficiency of converting the afterglow kinetic energy into radiation. As can be seen also in **Figure 10**, the isotropic equivalent energy that is radiated at optical wavelengths is ~2 orders of magnitude smaller than that in X-rays and γ-rays. This is predominantly due

to the fact that νF_ν typically peaks closer to the X-rays than to the optical, and it is very flat above its peak but falls much faster toward lower energies. Finally, because these are isotropic equivalent energies, most of the contribution to the radiated afterglow energy, especially at radio wavelengths, is from significantly later times than for $E_{X,iso}$, and the collimation of the outflow along with relativistic beaming effects could result in much larger $E_{X,iso}$ than the R-band isotropic energy $E_{R,iso}$.

Of the three nearby supernova-GRB events plotted in **Figure 10**, only GRB030329 falls within the $\sim 10^{50}$ erg range; the other two events fall between $\sim 10^{48}$ and $\sim 10^{49}$ erg (Kaneko et al. 2007). We note a selection effect (Malmquist bias) based on the observed photon flux: An event is more likely to be detected when it is closer to us than farther, for a given intrinsic luminosity.

One of the liveliest debates associated with GRBs concerns the total energy released during the explosion: Are GRBs standard candles? The GRB community has vacillated from initially claiming that the GRB intrinsic luminosity distribution was very narrow (Horack et al. 1994) to discounting all standard-candle claims, to accepting a standard total GRB energy of $\sim 10^{51}$ ergs (Frail et al. 2001), and to diversifying GRBs into normal and subenergetic classes (Ramirez-Ruiz et al. 2005a, Soderberg et al. 2008). The important new development is that we now have significant observational support for the existence of a subenergetic population based on the different amounts of relativistic energy released during the initial explosion. A network of theoretical tests lends credence to this idea (Granot & Ramirez-Ruiz 2004, Waxman 2004a, Granot & Kumar 2006, Pian et al. 2006, Kaneko et al. 2007). The existence of a wide range of intrinsic energies could further challenge the use of GRBs as standard candles.

4. ENVIRONMENTS AND HOST GALAXIES

Much of what we know about GRBs has been derived not from observations of the prompt burst radiations themselves but from studies of their afterglows—as they illuminate the circumburst surroundings—and their host galaxies. In this section, we discuss the primary insights that have been derived in this manner.

4.1. Cosmological Setting

Figure 4 presents the redshift distribution of all *Swift*-detected GRBs. *Swift* and other current missions observe GRBs to cosmological distances quite readily; indeed, the three highest-fluence, known-redshift bursts observed by *Swift* have been at $z = 0.61$ (GRB050525A), $z = 2.82$ (GRB050603), and $z = 1.26$ (GRB061007)—already spanning 40% of cosmic history. Historically, the majority of redshifts have been collected via host-galaxy spectroscopy; in the *Swift* era, however, this pattern has been reversed—except for the short bursts—with the great majority of redshifts now being derived from afterglow spectra. In addition to theoretical arguments that posit different physical origins for short and long bursts (e.g., Katz & Canel 1996), the absence of short-burst-associated supernovae to deep limits (Castro-Tirado et al. 2005, Fox et al. 2005, Hjorth et al. 2005a, Bloom & Prochaska 2006), 100 times fainter than SN1998bw in the best cases, argues for a distinct origin of the short and long bursts. In agreement with this picture, the redshift distributions of the two populations are not consistent.

For the long bursts, which are associated with active star formation and, in particular, the deaths of massive stars, it is interesting to explore whether their distribution in redshift is consistent with other measures of cosmic star formation. The greatly increased number of redshifts available for *Swift* bursts has motivated several such comparisons and, for the first time, estimates of cosmic star formation at high redshift ($z > 4$) using the *Swift* redshift sample (Chary, Berger & Cowie 2007; Yksel et al. 2008).

The star-formation studies over $1 < z < 4$ confirm, in a broad sense, that the GRB redshift distribution remains consistent with independent measures of star formation (Jakobsson et al. 2006). However, there are signs of differential evolution of the GRB rate, in the sense that the GRB rate increases more rapidly with increasing redshift than expected based on star-formation measures alone (Guetta & Piran 2007, Le & Dermer 2007, Kistler et al. 2008). This evidence, currently at roughly 95% confidence, may strengthen significantly in coming years. If so, it would provide a sign of bias toward low-mass and low-metallicity host galaxies—and potentially, low-metallicity progenitors—for the long-duration bursts (Section 4.2). The theoretical curves accompanying the GRB redshift distribution (**Figure 4**), which show the evolution of a comoving volume element in the Universe, and the volume convolved with star-formation rate, appear to indicate that the observed distribution is wider than expected.

The short-burst redshift distribution, so far drawn exclusively from host-galaxy observations, has also been compared to star-formation metrics. In this case, however, the intent has been to explore "time-delayed" progenitor models that correlate with star formation through a parametrized (log-normal or power-law) delay function (Guetta & Piran 2006; Nakar, Gal-Yam & Fox 2006; Salvaterra et al. 2008). Consistent with the relatively large fraction of events at $z \lesssim 0.5$ compared to long bursts, and with host-galaxy demographics (Shin & Berger 2007, Zheng & Ramirez-Ruiz 2007), these studies have concluded that a long-lived ($\tau \gtrsim 1$ Gyr) progenitor is required for these models to be consistent with *Swift*-era redshift measurements and the distribution of short-burst fluences from BATSE. This in turn has led to relatively high estimates of the volumetric local short-burst rate, at least an order of magnitude greater than the local rate of long bursts (Guetta, Granot & Begelman 2005), and a correspondingly optimistic set of predictions for Enhanced LIGO (Laser Interferometer Gravitational Wave Observatory), VIRGO, and other ground-based gravity-wave detectors.

4.2. Host Galaxies of Long Bursts

Surveys of GRB host galaxies in the pre-*Swift* era (Fynbo et al. 2003, Le Floc'h et al. 2003) necessarily focused on the host galaxies of long-duration bursts. These surveys established a standard picture for the GRB hosts as sub-L^* galaxies (median $L \sim 0.1\ L^*$) with exponential-disk light profiles (Conselice et al. 2005; Wainwright, Berger & Penprase 2007) and high specific star-formation rates (SSFR $\sim 1\ \mathrm{Gyr}^{-1}$) (Christensen, Hjorth & Gorosabel 2004). A selection of GRB host galaxies, as imaged by the *Hubble Space Telescope* (HST), is shown in **Figure 11**.

This picture has not substantially changed in the *Swift* era. To the contrary, the results of various ground- and space-based efforts to characterize GRB host galaxies (Le Floc'h et al. 2006; Chary, Berger & Cowie 2007; Fynbo et al. 2008; Savaglio, Glazebrook & LeBorgne 2009) have confirmed this basic outline and expanded its domain of applicability to high redshift, combining the power of the *Swift* burst catalog with Spitzer observations. At higher redshifts, $z \gtrsim 3$, it seems particularly interesting to use the GRB host galaxies to explore the evolution of mass-metallicity relationships that are typically compiled using field galaxies at low redshift and high-mass galaxy samples at high redshift (**Figure 12**). Because GRB host redshifts are typically secured via afterglow spectroscopy, the hosts themselves are uniquely free of mass and luminosity selection effects. In this context, even upper limits provide useful constraints on mass-metallicity correlations and their evolution with redshift (Chary, Berger & Cowie 2007; Berger 2009; Savaglio, Glazebrook & LeBorgne 2009). Such studies have also served to place GRB host galaxies in the context of other high-redshift galaxy populations, incuding the Lyman-break and Lyman-alpha (Ly α)–emitting galaxies (Fynbo et al. 2008).

Finally, it is somewhat reassuring that numerical simulations of star-forming galaxy populations can generate galaxy subpopulations that reproduce the basic properties of the GRB host

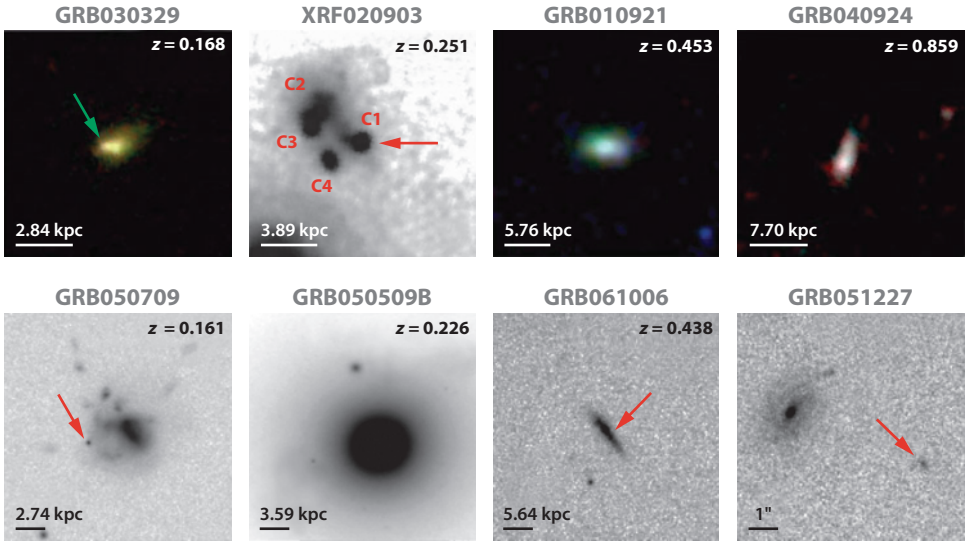

Figure 11

A selection of the host galaxies of long-duration (*top row*) and short-duration (*bottom row*) γ-ray bursts, as imaged by the *Hubble Space Telescope*. An attempt has been made to choose pairs of long- and short-burst host galaxies with comparable redshifts; lower-redshift hosts are emphasized because these reveal their structure more readily in short exposures. Images are oriented with north up and east to the left, and the physical length scale for a one-arcsecond angular distance is indicated in each panel (except for GRB051227); arrows point to the location of the burst where this is known to approximately pixel precision. Individual burst notes: GRB030329 was the first classical long GRB to be associated with a well-observed spectroscopic supernova (Hjorth et al. 2003, Stanek et al. 2003); XRF020903 was the first X-ray flash event to yield a redshift measurement (Soderberg et al. 2004); GRB050709 was the first short burst with optical afterglow—indicated by the arrow—detected (Fox et al. 2005, Hjorth et al. 2005b); GRB050509B was the first short burst with detected afterglow (Gehrels et al. 2005, Bloom et al. 2006); GRB051227 has a faint candidate host, of unknown redshift probably >1, visible at the optical afterglow location; the spiral galaxy to the east has redshift $z = 0.714$ (Foley et al. 2005). Long-burst host images from Wainwright, Berger & Penprase (2007); short-burst host images from Fox et al. (2005) and this review.

galaxies in several important respects (Courty, Björnsson & Gudmundsson 2004, 2007). In particular, selecting for high specific star-formation rate generates mock galaxy catalogs with masses, luminosities, and colors similar to those of GRB host galaxies.

4.2.1. Metallicity matters. Although GRB host galaxies are often studied for the insights they provide about larger astrophysical questions, including the history of star formation through cosmic time, they also have the potential to shed light on the nature of the GRB progenitors. The association of long-duration bursts with star formation, for example, was proposed after observation of just two host galaxies (Paczyński 1998) and was demonstrated firmly from the properties of the first twenty (Bloom, Kulkarni & Djorgovski 2002).

Recent years have seen a surge of interest in the question of whether GRB host galaxies, and hence, presumably, GRB progenitors, are metal-poor by comparison to the larger population of star-forming galaxies. This question has been explored from a variety of perspectives, and the result of these studies, still under active debate, may eventually help refine our picture of the massive stellar death behind each GRB.

The metallicities of GRB host galaxies, and indeed, detailed abundance profiles, can be measured directly from high-resolution spectroscopy of bright afterglows. This area has seen dramatic

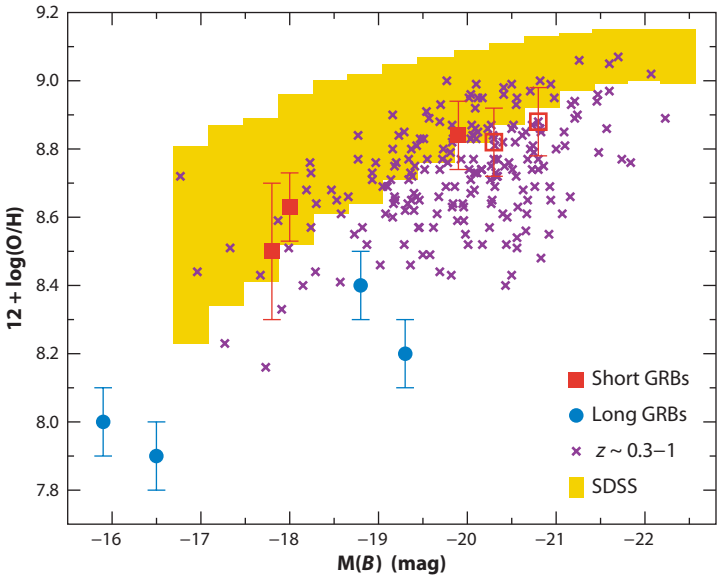

Figure 12

Metallicity as a function of *B*-band absolute magnitude for the host galaxies of short (*red*) and long (*blue*) GRBs. The yellow bars mark the 14–86 percentile range for galaxies at $z \sim 0.1$ from the Sloan Digital Sky Survey (Tremonti et al. 2004), whereas crosses designate field galaxies at $z \sim 0.3$–1 (Kobulnicky & Kewley 2004). Both field samples exhibit a clear luminosity-metallicity relation. The long GRB hosts tend to exhibit lower-than-expected metallicities (Stanek et al. 2006), whereas the hosts of short GRBs have higher metallicities by ∼0.6 dex and are moreover in excellent agreement with the luminosity-metallicity relation. From Berger (2009).

progress in the *Swift* era, with prompt arcsecond positions and visual magnitude measurements from *Swift* UVOT and ground-based robotic telescopes feeding rapid-response spectroscopy from large-aperture facilities. One chief result of these efforts has been the collection of detailed abundance characterizations for multiple bursts (Vreeswijk et al. 2004; Chen et al. 2005, 2007, 2009; Fynbo et al. 2006a; Bloom et al. 2007; Price et al. 2007; Prochaska et al. 2007). In addition, the metallicities of GRB host galaxies have been measured via standard emission-line diagnostics (Stanek et al. 2006; Thöne et al. 2008; Savaglio, Glazebrook & LeBorgne 2009), where possible, and in some cases tentative conclusions have been drawn on the basis of cruder relations such as mass-metallicity metrics (Berger et al. 2007a) and host-galaxy luminosities and morphologies (Fruchter et al. 2006).

The conclusions of these studies have yet to be reconciled into a single coherent picture of the nature of the GRB host galaxies and their relationship to other low- and high-redshift galaxy populations. However, the wealth of data have served to resolve some associated issues. First, the metallicities of GRB host galaxies at $z \lesssim 1$ are significantly ($Z \sim 0.1 Z_{\odot}$) subsolar (Savaglio, Glazebrook & LeBorgne 2009), consistent with the subsolar metallicities measured for GRB host galaxies via absorption spectroscopy at $z \gtrsim 2$ (e.g., Chen et al. 2009). These subsolar metallicities are neither surprising nor unusual for galaxy populations at high redshift (Fynbo et al. 2008; Savaglio, Glazebrook & LeBorgne 2009); moreover, several candidate higher-metallicity hosts have been identified, although not yet confirmed (Fruchter et al. 2006, Berger et al. 2007a). At the same time, GRB host galaxies seem to be readily distinguished, in luminosity and morphology, from the host galaxies of core-collapse supernovae at similar redshifts (Fruchter et al. 2006), and

the host galaxies of the lowest-redshift $z \lesssim 0.2$ bursts have uniformly low metallicities that strongly distinguish them from the bulk of the low-redshift galaxy population (Stanek et al. 2006, Thöne et al. 2008), and indeed, from the host galaxies of nearby type Ibc supernovae (Modjaz et al. 2008).

These somewhat divergent findings might be reconciled in a picture where the GRB progenitors prefer (or require) a low-metallicity environment, since the increasing prevalence of such environments at $z \gtrsim 1$ would allow GRB host galaxies to present an increasingly fair sample of the population of star-forming galaxies at these higher redshifts. This argument would also dovetail with observations that the GRB rate seems to increase with redshift faster than the cosmic star-formation rate, as mentioned above (Guetta & Piran 2007, Le & Dermer 2007, Kistler et al. 2008). However, the claim that GRB host galaxies represent a fair sample of star-forming galaxies, even at $z \gtrsim 1$, remains in dispute (e.g., **Figure 12**; Berger 2009).

A possibly significant implication of a metallicity-dependent GRB rate would be an offset between the true star-formation rate and that traced by GRBs. If GRBs in low-metallicity environments and low-mass galaxies are more luminous, then they are likely overrepresented in GRB samples. Low-mass galaxies and galaxy outskirts have lower metallicity on average and thus may yield more (and/or more luminous) GRBs than do high-mass galaxies (Ramirez-Ruiz, Lazzati & Blain 2002b). As galaxy mass builds up through mergers, it is also possible that the highest-z GRBs could be systematically more luminous owing to their lower-mass host galaxies, an intriguing hypothesis given the extreme luminosities of some of the highest-redshift bursts of the *Swift* era, including GRB050904.

Finally, it is worth noting that high-resolution afterglow spectra show absorption features imprinted on the afterglow by gas at multiple, widely divergent physical scales, possibly extending from $d \sim 10$ pc to Gpc distances (Section 4.2.2). With the GRB metallicity question ultimately referring to the nature of the progenitor itself, searches for definitive signatures of the progenitor's stellar wind material (Möller et al. 2002, Mirabal et al. 2003, Schaefer et al. 2003, Bloom et al. 2007, Chen et al. 2007, Fox et al. 2008, Prochaska et al. 2008) should continue to be pursued and refined. At the same time, in discussing the host galaxies as a population, more common galaxy-integrated, emission-line diagnostics may better serve to place GRB hosts in the proper cosmological context.

4.2.2. Subgalactic environments. The same fast-response spectra that have enabled characterization of elemental abundances in GRB host galaxies have led to a series of discoveries regarding absorbing gas structures on subgalactic scales within the GRB host: a rich array of high-ionization fine-structure Fe transitions in GRB051111 (Berger et al. 2005a; Penprase et al. 2006; Prochaska, Chen & Bloom 2006); discovery of time-variability of such fine-structure features in three bursts, demonstrating excitation by UV photons from the burst flash and young afterglow (Della Valle et al. 2006b, Vreeswijk et al. 2007, D'Elia et al. 2009); discovery of high-ionization Nv features, providing evidence for absorption by gas within $d \lesssim 10$ pc of the burst (Fox et al. 2008, Prochaska et al. 2008); and most recently, the first detection of molecular gas along the line of sight to a GRB afterglow (**Figure 13**; Prochaska et al. 2009).

The range of these discoveries reveals a surprising complication in the interpretation of afterglow spectra. Depending on the burst, it may be necessary to account for absorbing structures on every scale—the immediate parsec-size circumburst environment, the surrounding or intervening molecular clouds, the host-galaxy absorbers on kiloparsec scales, and ultimately low-ionization gas associated with cosmological structures at gigaparsec distances. Similar complications are a feature of quasar absorption line studies; there, however, the situation is simplified by the persistent nature and overwhelming ionizing power of the quasar itself.

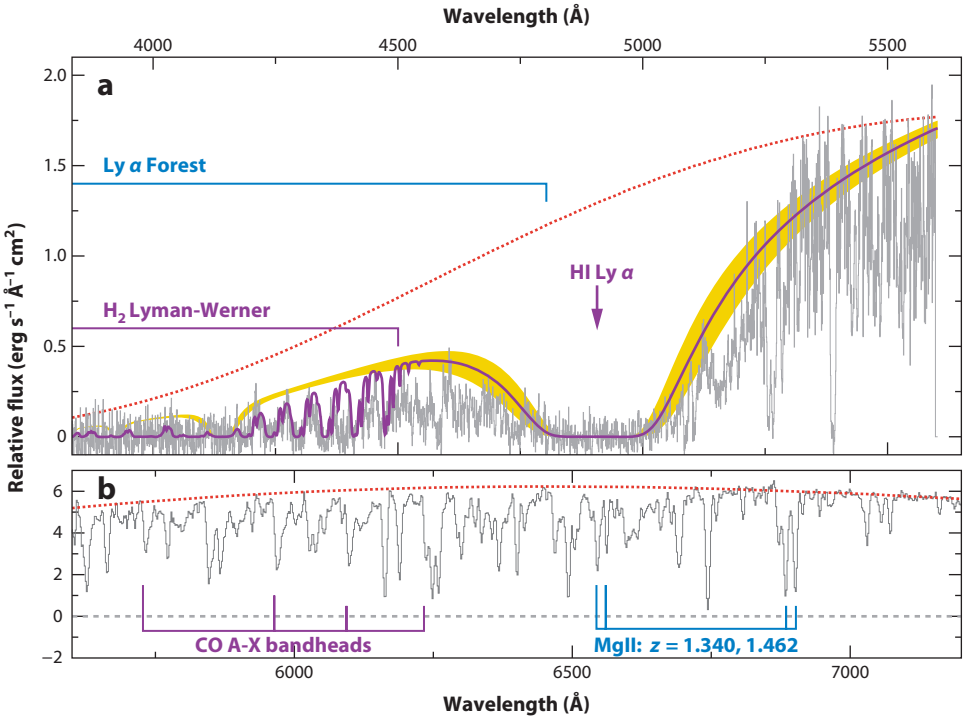

Figure 13

(*a*) Keck/LRIS spectrum of the afterglow for GRB080607 (Prochaska et al. 2009). The red dashed lines indicate a model of the intrinsic afterglow spectrum reddened heavily by dust in the host galaxy (rest-frame $A_V \approx 3.2$). At $\lambda \approx 4900$ Å, one identifies a damped Lyman-alpha (Ly α) profile associated with HI gas near the GRB. The yellow shaded region overplotted on the gray data corresponds to an HI column density $N_H = 10^{22.7\pm0.15}$ cm^{-2}. The model (*purple solid line*) includes absorption from H_2 Lyman-Werner transitions. The line opacity at $\lambda > 5500$ Å is dominated by metal-line transitions from gas in the host galaxy and includes bandheads of the CO molecule. Surprisingly, this is the only sightline to date to show strong molecular absorption (Tumlinson et al. 2007). It also exhibits a roughly solar metallicity. (*b*) The spectral region or features corresponding to intergalactic Ly α and MgII absorption. The redshift for GRB080607 is $z = 3.036$.

Indeed, the situation may be even more complicated than this. The discovery that the frequency (dN/dz) of strong MgII absorbers along GRB lines of sight seems to be roughly four times the frequency along quasar lines of sight (Prochter et al. 2006) suggests that some or most such absorbers seen toward GRBs—despite their large separation in redshift from the host galaxy—may be intrinsic to the GRB environment (Porciani, Viel & Lilly 2007).

4.3. Host Galaxies of Short Bursts

At the time of the *Swift* launch, the greatest mystery in GRB astronomy was the origin of short GRBs. A major step forward was made in the summer of 2005 with the localization and afterglow detection of three short bursts, GRB050509B, GRB050709, and GRB050724. These events were found to be localized in regions of low star formation, either in low star-forming elliptical galaxies as for GRB050509B (Gehrels et al. 2005, Bloom et al. 2006) and GRB050724 (Barthelmy et al. 2005c, Berger et al. 2005b) or in a region of a galaxy with low star formation (Fox et al. 2005,

Hjorth et al. 2005b, Villasenor et al. 2005). This was in stark contrast to long bursts, which are associated with star-forming regions, and implied a nonmassive core-collapse origin.

More than three years after these first short-burst localizations, the catalog of confidently identified short-burst host galaxies is growing to the point where systematic studies can be carried out (Berger 2009)—although the effects of uncertain burst attribution (i.e., long or short?), uncertain host identification (especially for bursts with only *Swift* BAT or XRT localizations), and unknown redshifts for faint candidate hosts keep any conclusions largely qualitative at this time.

Indeed, without direct afterglow spectroscopy, association of short bursts with candidate host galaxies and host-galaxy clusters must be approached probabilistically. In cases where a well-localized (preferably subarcsecond) afterglow falls on a luminous region of the candidate host, or within a high-mass or high-redshift cluster, the association can probably be considered secure; however, in other cases an a posteriori estimate of the probability of association must be made (Bloom & Prochaska 2006, Fox & Roming 2007). Such estimates are inevitably strongly dependent on input assumptions. For example, what lifetime and kick-velocity distributions might be appropriate for progenitor binary systems? What about other possible progenitor classes? Any assumptions must be carefully considered before and after they are applied.

With these caveats, a picture of the short-burst host-galaxy population as a whole has developed (**Figure 11**). It consists of three classes of host, two of which became apparent soon after the short-burst afterglow revolution of 2005: the low-redshift ($z < 0.5$), high-mass ($L \sim L^*$), early-type host galaxies and galaxy clusters, on the one hand (Berger et al. 2005b, Fox et al. 2005, Gehrels et al. 2005, Bloom et al. 2006, Gal-Yam et al. 2008), typified by the hosts of GRB050509B, GRB050724, and GRB050813; and the low-redshift, sub-L^*, late-type galaxies on the other, typified by the hosts of GRB050709 (Fox et al. 2005, Covino et al. 2006), GRB051221 (Soderberg et al. 2006a), and GRB061006 (D'Avanzo et al. 2009).

The third class of short-burst host galaxies consists of faint, star-forming galaxies at $z \gtrsim 1$ (Berger et al. 2007b, Cenko et al. 2009, Berger 2009), reminiscent of the host galaxies of long bursts. The existence of such higher-redshift, star-forming, short-burst host galaxies was predicted (Belczynski et al. 2006) on the basis of binary population synthesis models assuming the compact object merger model for the short bursts. These simulations yield a bimodal distribution of lifetimes for merging systems, with a spike of mergers at short time scales, $\tau \lesssim 100$ Myr, followed by a dominant merger population with a τ^{-1} lifetime distribution. The association of short GRBs with both star-forming and early-type galaxies has led to analogies with type Ia supernovae, whose host demographics have similarly provided evidence for a wide distribution of delay times between formation and explosion. At the same time, both core-collapse supernovae and long-duration GRBs are observed (almost) exclusively in late-type star-forming galaxies. As with supernovae and long-duration bursts, a detailed census of short-burst redshifts, host-galaxy types, and burst locations within those hosts will undoubtedly help to constrain progenitor models.

4.4. Neither Long Nor Short

Some interesting GRB host galaxies are not obviously associated with either the long or short burst classes. In fact, the "peculiar" cases of GRB060505 and GRB060614 probably provide the first examples where studies of the host-galaxy properties have been applied to argue for a (long- or short-) nature of the bursts themselves (Fynbo et al. 2006b, Gal-Yam et al. 2006, Ofek et al. 2007, Thöne et al. 2008).

GRB060614 was a low-redshift, long-duration burst with no detection of a coincident supernova to deep limits. It was a bright burst (fluence in the 15–150 keV band of 2.2×10^{-5} erg cm^{-2}) and well studied in the X-ray and optical. With a T90 duration of 102 s, it seems to fall squarely

in the long-burst category. A host galaxy was found (Della Valle et al. 2006a, Fynbo et al. 2006b, Gal-Yam et al. 2006) at $z = 0.125$ and deep searches were made for a coincident supernova. All other well-observed nearby GRBs have had supernovae detected, but this one did not to limits >100 times fainter than previous detections.

GRB060614 shares some characteristics with short bursts (Gehrels et al. 2006). The BAT light curve shows a first short, hard-spectrum episode of emission (lasting 5 s) followed by an extended and somewhat softer episode (lasting ∼100 s). The total energy content of the second episode is five times that of the first. Its light-curve shape is similar in many respects to that of short bursts with extended emission. There are, however, differences: The short episode of this event is longer than in the previously detected examples, and the soft episode is relatively brighter. Another similarity with short bursts comes from a lag analysis of GRB060614. The lag between temporal structures in the 50–100 keV band and those in the 15–25 keV bands for the first 5 s is 3 ± 6 ms, which falls in the same region of the lag-luminosity plot as short bursts (**Figure 5**). It is difficult to determine unambiguously which category of burst GRB060614 falls into. It is a long event by the traditional definition, but it lacks an associated supernova as had been observed in all other nearby long GRBs. It shares some similarities with *Swift* short bursts but also has important differences, such the brightness of the extended soft episode. If it is due to a collapsar, it is the first indication that some massive star collapses either fail as supernovae (Woosley 1993) or highly underproduce ^{56}Ni (Lopez-Camara, Lee & Ramirez-Ruiz 2009); if it is due to a merger, then the bright, long-lived soft episode is hard to explain within the framework of compact binary mergers (Di Matteo, Perna & Narayan 2002; Lee, Ramirez-Ruiz & Page 2004; Setiawan, Ruffert & Janka 2004). Thus, this peculiar burst has challenged the usual classifications of GRBs.

5. BASIC PHYSICAL CONSIDERATIONS

In this section, we endeavor to outline some of the physical processes that are believed to be most relevant to interpreting GRBs. Although the field is far from maturity, sufficient progress has been made in identifying the essential physical ingredients. A basic scheme can provide a conceptual framework for describing the observations even when the framework is inaccurate. The following should be interpreted in this spirit.

GRB activity manifests itself over a dynamical range of ∼13 decades in radius. **Figure 14** shows a schematic montage of successive decades, exhibiting phenomena that are believed to take place on each of these length scales. The phenomena are not directly observed, and the associated frames represent educated guesses of their geometrical arrangements. An anatomical summary of the underlying physical processes, working outward from the smallest to the largest scales, follows.

5.1. The Central Engine

In principle, flow onto a compact object can liberate gravitational potential energy at a rate approaching a few tenths of $\dot{M}c^2$, where $\dot{M}$ is the mass inflow rate. Even for such high efficiencies the mass requirements are rather large, with the more powerful GRB sources ($\sim 10^{53}$ erg s^{-1}) having to process more than $10^{-2}\ M_\odot$ s^{-1} through a region only slightly larger than a NS or a stellar-mass BH. Radiation of the BH rest mass on a time scale r_g/c, where $r_g = GM/c^2 = 1.5 \times 10^5 (M/M_\odot)$ cm is the characteristic size of the collapsed object, would yield luminosities $c^5/G = 4 \times 10^{59}$ erg s^{-1}.

When mass accretes onto a BH or NS under these conditions, the densities and temperatures are so large that photons are completely trapped, and neutrinos, being copiously emitted, are the main source of cooling. The associated interaction cross section is then many orders of magnitude smaller, and, as a result, the allowed accretion rates and luminosities are correspondingly much

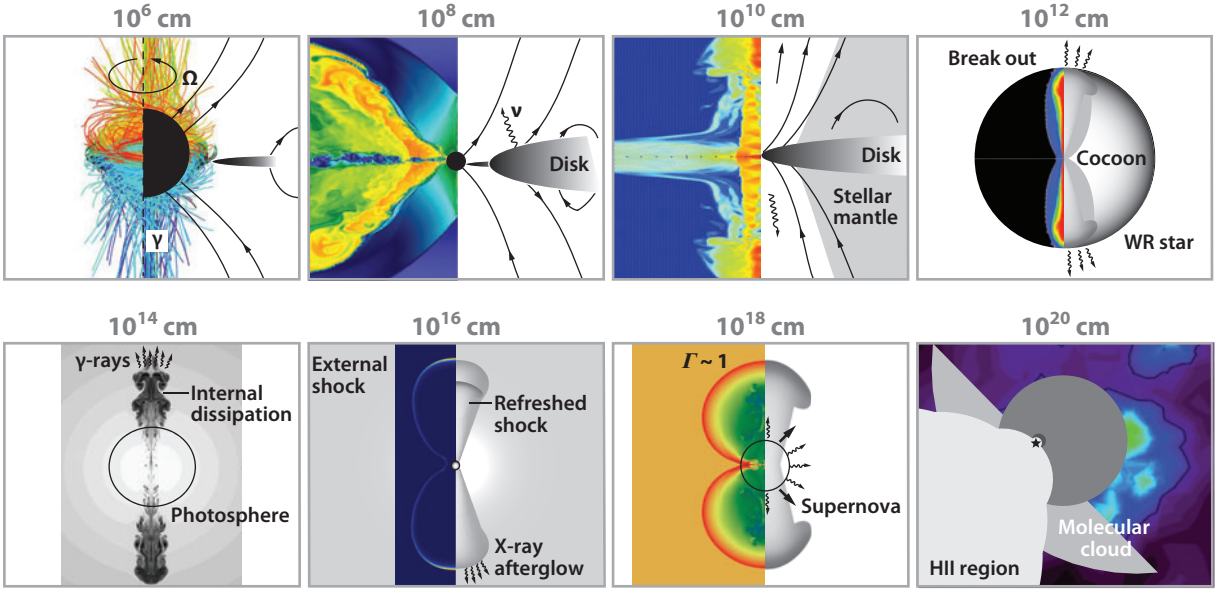

Figure 14

Diagram exhibiting GRB activity over successive decades in radius ranging from 10^6 cm to 1 pc. The first task in attempting to construct a general scheme of GRBs is to decide which parameters exert a controlling influence upon their properties. (10^6 cm) The GRB nucleus (BH or NS) and its magnetosphere. (10^8 cm) The accretion flow is likely to be embedded in a very active corona. We expect coronal arches, as well as large magnetic structures, to be quite common and to be regenerated on an orbital timescale. Relativistic outflow from the black hole is proposed to be focused into two jets. (10^{10} cm) Even if the outflow is not narrowly collimated, some beaming is expected because energy would be channeled preferentially along the rotation axis. The majority of stellar progenitors, with the exception of some very compact stars, will not collapse entirely during the typical duration of a GRB. A stellar envelope will thus remain to impede the advance of the jet. (10^{12} cm) This is the typical size of an evolved massive star progenitor. A thermal break-out signal should precede the canonical, softer γ-rays observed in GRBs. (10^{14} cm) Velocity differences across the jet profile provide a source of free energy. The most favorable region for shocks producing highly variable γ-ray light curves is above the baryonic or pair-dominated photosphere. (10^{16} cm) The external shock becomes important when the inertia of the swept-up external matter starts to produce an appreciable slowing down of the ejecta. (10^{18} cm) Finally, we come to the end of the relativistic phase. This happens when the mass E/c^2 has been swept-up.

higher. For example, using the cross section for neutrino pair production [although we have considered here the specific case of neutrino pair creation, the estimates vary little when one considers, for example, coherent scattering of neutrinos by nuclei and/or free nucleons (except for the energy scaling)], the Eddington limit can be rewritten as $L_{\mathrm{Edd},\nu} = 8\times10^{53}(E_\nu/50\,\mathrm{MeV})^{-2}(M/M_\odot)\,\mathrm{erg\,s^{-1}}$, with an associated accretion rate is of $\dot{M}_{\mathrm{Edd},\nu}\times(\mathrm{efficiency})^{-1}$, where $\dot{M}_{\mathrm{Edd},\nu} = L_{\mathrm{Edd},\nu}/c$ (Ramirez-Ruiz 2006b, Lee & Ramirez-Ruiz 2007).

The blackbody temperature if a luminosity $L_{\mathrm{Edd},\nu}$ emerges from a sphere of radius r_g (similar overall fiducial numbers also hold for neutron stars, except that the simple mass scalings obtained here are lost) is

$$T_{\mathrm{Edd},\nu} = \left(\frac{L_{\mathrm{Edd},\nu}}{4\pi r_{\mathrm{g}}^2\sigma_{\mathrm{SB}}}\right)^{1/4} \sim 45\,(M/M_\odot)^{-1/4}\left(\frac{E_\nu}{50\,\mathrm{MeV}}\right)^{-1/2}\ \mathrm{MeV}. \qquad (1)$$

The radiation temperature is expected to be $\leq T_{\mathrm{th}} = GMm_{\mathrm{p}}/(3kr_{\mathrm{g}}) \sim 200$ MeV, the temperature the accreted material would reach if its gravitational potential energy were turned entirely into thermal energy.

Related to this, there is a fiducial density in the vicinity of the BH

$$\rho_{\mathrm{Edd},\nu} = \frac{\dot{M}_{\mathrm{Edd},\nu}}{4\pi r_{\mathrm{g}}^2 c} \sim 10^{11}(M/M_{\odot})^{-1}\left(\frac{E_\nu}{50\,\mathrm{MeV}}\right)^{-2}\ \mathrm{g\,cm^{-3}}. \quad (2)$$

It should be noted that the typical Thomson optical depth under these conditions is $\tau_{\mathrm{T}} \sim n_{\mathrm{Edd},\nu}^{1/3} r_{\mathrm{g}} \sim 10^{16}$ and so, as expected, photons are incapable of escaping and constitute part of the fluid. A characteristic magnetic field strength is that for which $B^2/8\pi = n_{\mathrm{Edd},\nu} m_p c^2$:

$$B_{\mathrm{Edd},\nu} = \left(\frac{L_{\mathrm{Edd},\nu}}{r_g^2 c}\right)^{1/2} \sim 3 \times 10^{16}(M/M_{\odot})^{11/2}\left(\frac{E_\nu}{50\,\mathrm{MeV}}\right)^{-1}\ \mathrm{G}. \quad (3)$$

If a field $B_{\mathrm{Edd},\nu}$ were applied to a BH with $J \approx J_{\max}$, the electromagnetic power extraction would be $\sim L_{\mathrm{Edd},\nu}$ (Usov 1992).

5.2. Accretion Flows

As we discussed above, a BH or NS embedded in infalling matter offers a more efficient power source than any other conceivable progenitor. Although this efficiency is over a hundred times larger than that traditionally associated with thermonuclear reactions, the required rate of mass supply for a typical GRB is of course colossal. Such high mass-fueling rates are never reached for BHs in XRBs or active galactic nuclei, where the luminosity remains well below the photon Eddington limit. They can, however, be achieved in the process of forming NSs and stellar-mass BHs during the collapse of massive stellar cores (Houck & Chevalier 1991; Woosley 1993; MacFadyen & Woosley 1999; Narayan, Piran & Kumar 2001) and in binary mergers involving compact objects (Ruffert et al. 1997; Kluzniak & Lee 1998; Rosswog & Liebendörfer 2003; Rosswog, Speith & Wynn 2004; Lee, Ramirez-Ruiz & Page 2005; Setiawan, Ruffert & Janka 2006; Metzger, Piro & Quataert 2008). Consequently, most recent theoretical work has been directed toward describing the possible formation channels for these systems (Fryer, Woosley & Hartmann 1999; Belczynski, Bulik & Rudak 2002; Izzard, Ramirez-Ruiz & Tout 2004; Podsiadlowski et al. 2004). This involves evaluating those that are likely to produce a viable central engine and understanding the flow patterns near relativistic objects accreting matter in the hypercritical regime (Di Matteo, Perna & Narayan 2002; Perna, Armitage & Zhang 2006; Proga & Zhang 2006; Chen & Beloborodov 2007; Shibata, Sekiguchi & Takahashi 2007; Kumar, Narayan & Johnson 2008), where photons are unable to provide cooling but neutrinos do so efficiently.

The angular momentum is generally a crucial parameter, in many ways determining the geometry of the flow (Lee & Ramirez-Ruiz 2006). The quasi-spherical approximation breaks down when the gas reaches a radius $r_{\mathrm{circ}} \sim l^2/GM$, where l is the angular momentum per unit mass, and if injection occurs more or less isotropically at large radii, a familiar accretion disk will form. The inner regions of disks with mass fluxes $\leq \dot{M}_{\mathrm{Edd},\nu}$ are generally able to cool by emitting neutrinos on timescales shorter than the inflow time.

If $\dot{m} = \dot{M}/\dot{M}_{\mathrm{Edd},\nu} \leq 1$, then the bulk of the neutrino radiation comes from a region only a few gravitational radii in size, and the physical conditions can be scaled in terms of the Eddington quantities defined above. The remaining relevant parameter, related to the angular momentum, is $v_{\mathrm{inflow}}/v_{\mathrm{freefall}}$, where $v_{\mathrm{freefall}} \simeq (2GM/r)^{1/2}$ is the freefall velocity. The inward drift speed v_{inflow} would be of order v_{freefall} for supersonic radial accretion. When angular momentum is important, this ratio depends on the mechanism for its transport through the disk, which is related to the effective shear viscosity. For a thin disk, the factor $(v_{\mathrm{inflow}}/v_{\mathrm{freefall}})$ is of order $\alpha(H/r)^2$, where H is the scale height at radius r and α is the phenomenological viscosity parameter (Shakura

& Syunyaev 1973). The characteristic density, at a distance r from the hole, taking account of the effects of rotation, is

$$\rho \sim \dot{m}(r/r_g)^{-3/2}(v_{\rm inflow}/v_{\rm freefall})\rho_{{\rm Edd},\nu}, \quad (4)$$

and the maximum magnetic field, corresponding to equipartition with the bulk kinetic energy, would be

$$B_{\rm eq} \sim \dot{m}^{1/2}(r/r_g)^{-5/4}(v_{\rm inflow}/v_{\rm freefall})^{1/2}\, B_{{\rm Edd},\nu}. \quad (5)$$

Any neutrinos emerging directly from the central core would have energies of a few MeV. Note that, as mentioned above, $kT_{{\rm Edd},\nu}$ is far below the virial temperature $kT_{\rm vir} \simeq m_p c^2(r/r_g)$. The flow pattern when accretion occurs would then be determined by the value of the parameters $L_\nu/L_{{\rm Edd},\nu}$, which determine the importance of radiation pressure and gravity, and the ratio $t_{\rm cool}/t_{\rm dynamical}$, which fixes the temperature if a stationary flow pattern is set up.

It is widely believed that accretion onto a compact object, be it a NS or a stellar-mass BH, offers the best hope of understanding the "prime mover" in all types of GRB sources, although a possible attractive exception includes a rapidly spinning NS with a powerful magnetic field (Usov 1992; Thompson 1994; Spruit 1999; Thompson, Chang & Quataert 2004; Uzdensky & MacFadyen 2007; Bucciantini et al. 2008; Dessart et al. 2008). If there is an ordered field B, and a characteristic angular velocity ω, for a spinning compact source of radius r_*, then the magnetic dipole moment is $\sim Br_*^3$. General arguments suggest (Pacini 1967, Gold 1968) that the nonthermal magnetic-dipole-like luminosity will be $L_{\rm em} \approx B^2 r_*^6 \omega^4/c^3$, and simple scaling from these familiar results of pulsar theory require fields of order 10^{15} G to carry away the rotational or gravitational energy (which is $\sim 10^{53}$ erg) in a time scale of seconds (Usov 1992).

5.3. Jet Production

There are two ingredients necessary for the production of jets. First, there must be a source of material with sufficient free energy to escape the gravitational field of the compact object. Second, there must be a way of imparting some directionality to the escaping flow. Our eventual aim must be to understand the overall flow pattern around a central compact object, involving accretion, rotation, and directional outflow, but we are still far from achieving this. Most current workers who have discussed outflow and collimation have simply invoked some central supply of energy and material. A self-consistent model incorporating outflow and inflow must explain why some fraction of the matter can acquire a disproportionate share of energy (i.e., a high enthalpy).

A spinning BH (or NS) constitutes an excellent gyroscope, and the ingredients of accretion, angular momentum, entropy production, and possibly magnetic fields are probably sufficient to ensure the production of collimated outflow (McKinney 2006). However, the detailed mechanism is a matter for debate (it is not even clear what is accelerated), and several distinct lines of research are currently being pursued. One solution is to reconvert some of this energy via collisions outside the disk into electron-positron pairs or photons (Goodman, Dar & Nussinov 1987; Mochkovitch et al. 1993; Rosswog & Ramirez-Ruiz 2002; Rosswog, Ramirez-Ruiz & Davies 2003; Aloy, Janka & Möller 2005; Dessart et al. 2009). If this occurs in a region of low baryon density (e.g., along the rotation axis, away from the equatorial plane of the disk), a relativistic pair-dominated wind can be produced. An obvious requirement for this mechanism to be efficient is that the neutrinos escape (free streaming, or diffusing out if the density is high enough) in a time scale shorter than that for advection into the BH. The efficiency for conversion into pairs (scaling with the square of the neutrino density) is too low if the neutrino production is too gradual, so this can become a delicate balancing act.

Jets may alternatively be produced electromagnetically. Such a mechanism could, in principle, circumvent the above restriction on efficiency. The potential difference across a disk threaded by open magnetic field lines can exceed 10^{22} V, and this is available for accelerating high-energy particles, which will produce an electron-positron cascade and ultimately a relativistic jet that carries away the binding energy of the accreting gas. Blandford & Znajek (1977) extended this idea to BHs and showed how the spin energy of the BH could likewise be extracted. A hydromagnetic description of this mechanism is more likely to be appropriate (Blandford & Payne 1982). The field required to produce $L_{\rm em} \geq 10^{51}$ erg s^{-1} is enormous and may be provided by a helical dynamo operating in hot, convective nuclear matter with a millisecond period (Duncan & Thompson 1992). A dipole field of the order of 10^{15} G appears weak compared to the strongest field (Thompson, Quataert & Burrows 2005; Price & Rosswog 2006) that can in principle be generated by differential rotation ($\sim 10^{17}[P/1\,{\rm ms}]^{-1}$ G), or by convection ($\sim 10^{16}$ G), although how this may come about is not resolved in detail. Note, however, that it only takes a residual torus (or even a cold disk) of $10^{-3}\,M_\odot$ to confine a field of 10^{15} G.

A potential death-trap for such relativistic outflows is the amount of entrained baryonic mass from the surrounding medium. For instance, a Poynting flux of 10^{53} erg could not accelerate an outflow to $\Gamma \geq 10^2$ if it had to drag more than $\sim 10^{-4}\,M_\odot$ of baryons with it. A related complication renders the production of relativistic jets even more challenging, because the high neutrino fluxes are capable of ablating baryonic material from the surface of the disk. Thus, a rest-mass flux $\dot{M}_\eta$ limits the bulk Lorentz factor of the wind to $\Gamma_\eta = L_{\rm wind}/(\dot{M}_\eta c^2)$. Assuming that the external poloidal field strength is limited by the vigor of the convective motions, the spin-down luminosity scales with neutrino flux as $L_{\rm wind} \approx L_{\rm em} \propto B^2 \propto v_{\rm con}^2 \propto L_\nu^{2/3}$, where $v_{\rm con}$ is the convective velocity. The ablation rate is $\propto L_\nu^{5/3}$ (Qian & Woosley 1996; Metzger, Thompson & Quataert 2007), which indicates that the limiting bulk Lorentz factor Γ_η of the wind decreases as L_ν^{-1}. Thus, the burst luminosity emitted by a magnetized neutrino cooled disk may be self-limiting. Mass loss could, however, be suppressed if the relativistic wind were somehow collimated into a jet. This suggests that centrifugally driven mass loss will be heaviest in the outer parts of the disk and that a detectable burst may be emitted only within a relatively small solid angle centered on the rotation axis (Levinson & Eichler 2000).

5.4. Jet Collimation, Stability, and Confinement

As we discussed above, one of the key issues concerning jets is how they are formed. A second one is how they retain their coherence and collimation as they traverse circumburst space. The second issue is no less pressing than the first, since jet-like flows known on Earth are notoriously unstable. The situation in a jet is nonetheless different from that encountered in the laboratory because of the super-Alfvénic and supersonic streaming velocity (McKinney & Blandford 2009). Magnetohydrodynamics (MHD) probably provides a better description of the macroscopic behavior of a GRB jet than in the case of laboratory plasmas because the particle Larmor radii are so much smaller than the transverse size of the jet. Formal stability analysis of even the simplest jet models is complex. Unstable MHD modes (including pinch and kink instability) do not grow as rapidly as in stationary plasma, although sufficiently short-wavelength unstable modes localized within the jet interior are not suppressed by the relative motion. Longitudinal magnetic field in the core of the jet can likewise act as a backbone, provided that the correlation length of the magnetic field reversal along the jet exceeds the wavelength of the perturbation. Instabilities may be suppressed for perturbations of large wavelength along the jet by the inertia of the ambient medium. Whatever one's view of the relative merits of fluid and electromagnetic models of relativistic jets—and perhaps the truth lies between the two extremes—it is clear that our understanding of the role of magnetic fields in jets is less advanced than that of other aspects of the problem.

An understanding of the collimation and confinement of a jet can come about only through knowledge of the properties of the medium through which it propagates. Information about the ambient pressure gradient propagates into the jet at the internal sound speed. If the jet moves through a background with pressure scale height $\sim r$, the necessary condition for the jet interior to remain in pressure balance with its surroundings is $\theta M_j \leq 2$, where M_j is the Mach number and $\theta \sim d/r$ is the opening angle. If this condition is not satisfied when a jet is moving into a region of higher pressure, then strong shocks are driven into the jet. A jet moving into a region of lower pressure becomes overpressured relative to its surroundings and thereafter expands freely.

Freedom or confinement? This is the first question for which an extrinsic or environmental effect comes into play (which may, in turn, strongly affect what we observe), and it is thought to be particularly important for massive stellar GRB progenitors. This is because in such stars, a stellar envelope will remain to impede the advance of the jet (MacFadyen & Woosley 1999; Aloy et al. 2000; MacFadyen, Woosley & Heger 2001; Mészáros & Rees 2001; Ramirez-Ruiz, Celotti & Rees 2002a; Matzner 2003; Proga et al. 2003; Zhang, Woosley & Heger 2004). The beam will then evacuate a channel out to some location where it impinges on the stellar envelope. A continuous flow of relativistic fluid emanating from the nucleus supplies this region with mass, momentum, energy, and magnetic flux. Most of the energy output during that period is deposited into a cocoon or "wastebasket" surrounding the jet, which, after expansion, would have enough kinetic energy to substantially alter the structure of the relativistic outflow, if not, in fact, provide much of the observed explosive power (Ramirez-Ruiz, Celotti & Rees 2002a).

Can relativistic jets really be formed inside stars? This is not the most propitious environment for the creation of an ultrarelativistic, baryon-starved jet. What needs to be demonstrated is that the outflow is not "poisoned" by baryons by the time it reaches the surface of the star. It appears that it is not necessary to collimate the jet very tightly or to achieve a high bulk Lorentz factor as the flow leaves the stellar surface (Zhang, Woosley & Heger 2004; Morsony, Lazzati & Begelman 2007). As long as the emergent flow has a high enthalpy per baryon, it will expand and achieve its high terminal speed some distance from the star (Uzdensky & MacFadyen 2007, Bucciantini et al. 2008). A strong thermal break-out signal is expected to precede the canonical γ-rays observed in GRBs with massive progenitors as the shock breaks through the stellar surface and exposes the hot shocked material (MacFadyen, Woosley & Heger 2001; Ramirez-Ruiz, MacFadyen & Lazzati 2002c; Waxman & Mészáros 2003; Waxman, Mészáros & Campana 2007). For very extended envelopes, the jet may be unable to break through the envelope. TeV neutrino signals produced by Fermi accelerated relativistic protons within the cork may provide a means of detecting such choked-off, γ-ray dark collapses (Mészáros & Waxman 2001).

5.5. Dissipation and Cooling Effects Within the Jet

The unique feature of GRBs is that the bulk Lorentz factor Γ may reach values from hundreds to thousands (Lithwick & Sari 2001). The relativistic motion of the radiating particles introduces many interesting effects in GRB emissions that must be properly taken into account (e.g., Fenimore, Madras & Mayakshin 1996).

Three frames of reference are considered when discussing the emission from systems moving with relativistic speeds: the stationary frame, which is denoted here by asterisks, the comoving frame, denoted by primes, and the observer frame. The differential distance traveled by the expanding source during differential time dt_* is $dr = \beta c\, dt_*$, where $\beta = \sqrt{1-\Gamma^{-2}}$. Due to time dilation, $dr = \beta\Gamma c\, dt'$. The relationship between comoving and observer times is $(1+z)\Gamma dt'(1-\beta\cos\theta) = (1+z)dt'/\delta = dt$, where θ is the angle between the emitting element and the observer, $\delta = [\Gamma(1-\beta\cos\theta)]^{-1}$ is the Doppler factor, and z is the cosmological redshift. For an on-axis observer therefore $dt \cong (1+z)dr/\Gamma^2 c$, and, as a result, the blast wave can travel a

large distance $\Gamma^2 c\,\Delta t$ during a small observing time interval. A photon detected with dimensionless energy $\epsilon = h\nu/m_e c^2$ is emitted with energy $\delta\epsilon'/(1+z)$.

Few would dispute the statement that the photons that bring us all our information about the nature of GRBs are the result of triboluminescence. For instance, velocity differences across the jet profile provide a source of free energy from particle acceleration through shock waves, hydromagnetic turbulence, and tearing mode magnetic reconnection (Rees & Mészáros 1994). If the value of Γ at the base increases by a factor ≥ 2 over a time scale Δt, then the later ejecta will catch up and dissipate a fraction of their energy at radius given by

$$r_\iota \sim c\,\Delta t \Gamma^2 \sim 3 \times 10^{14} \Delta t_0 \Gamma_2^2 \text{ cm}, \tag{6}$$

where $\Delta t = 1\Delta t_0$ s and $\Gamma = 10^2\Gamma_2$. Dissipation, to be most effective, must occur when the wind is optically thin: $\tau_T \simeq n'\sigma_T(r/\Gamma) \leq 1$ (here n' is the comoving number density). Otherwise it will suffer adiabatic cooling before escaping (Goodman 1986). The photosphere (baryonic or pair-dominated) is a source of soft thermalized radiation, which may be observationally detectable in some GRB spectra and may also result in inverse Compton cooling of the nonthermal electrons accelerated in the shocks occurring outside the photosphere (Mészáros & Rees 2000; Spada, Panaitescu & Mészáros 2000; Kobayashi, Ryde & MacFadyen 2002; Mészáros et al. 2002; Ramirez-Ruiz & Lloyd-Ronning 2002; Ramirez-Ruiz 2005; Pe'er, Mészáros & Rees 2006; Giannios & Spruit 2007; Thompson, Mészáros & Rees 2007; Ryde & Pe'er 2009).

In the presence of turbulent magnetic fields built up behind the shocks, the electrons can produce a synchrotron power-law radiation spectrum, whereas the inverse Compton scattering of these synchrotron photons extends the spectrum into the GeV range (Mészáros Rees & Papathanassiou 1994). To illustrate the basic idea, suppose that electrons, protons, and magnetic field share the available internal energy. Then the electrons reach typical random Lorentz factors of $\gamma \sim m_p/m_e$, and the assumption of a Poynting flux L_B implies a comoving magnetic field of order $B \sim L_B^{1/2} r_\iota^{-1}\Gamma^{-1} \sim 10^5 L_{B,50}^{1/2} r_{\iota,13}^{-1}\Gamma_2^{-1}$ G, where $L_B = 10^{50} L_{B,50}$ erg s^{-1} and $r_\iota = 10^{13} r_{\iota,13}$ cm. For these values of γ and B, the typical observed synchrotron frequency is $\nu_{sy} \sim 0.5 L_{B,50}^{1/2} r_{\iota,13}^{-1}(1+z)^{-1}$ MeV, independent of the bulk Lorentz factor Γ and in excellent agreement with the observed values of the νF_ν peak of GRB spectra (**Figure 1**). Yet, there are in some instances serious problems associated with this model (e.g., dissipation efficiencies). These difficulties have motivated consideration of alternative scenarios (e.g., Kumar & McMahon 2008, Kumar & Narayan 2009).

A magnetic field can ensure efficient cooling even if it is not strong enough to be dynamically significant. If, however, the field is dynamically significant in the wind (Mészáros & Rees 1997), then its internal motions could lead to dissipation even in a constant-velocity wind (Thompson 1994). Instabilities in this magnetized wind may be responsible for particle acceleration (Thompson 2006), and it is possible that γ-ray production occurs mainly at large distances from the source (Lyutikov & Blandford 2003).

A further effect renders the task of simulating unsteady winds even more challenging. This stems from the likelihood that any entrained matter would be a mixture of protons and neutrons. If a streaming velocity builds up between ions and neutrons, then interactions can lead to dissipation even in a steady jet where there are no shocks (Derishev, Kocharovsky & Kocharovsky 1999; Beloborodov 2003).

5.6. Jet Interaction with the External Environment

Astrophysicists understand supernova remnants reasonably well, despite continuing uncertainty about the initiating explosion; likewise, we may hope to understand the afterglows of GRBs, despite the uncertainties about the trigger that we have already emphasized.

In the simplest version of the afterglow model, the blast wave is approximated by a uniform thin shell. A forward shock is formed when the expanding shell accelerates the external medium, and a reverse shock is formed by deceleration of the cold shell. The forward- and reverse-shocked fluids are separated by a contact discontinuity and have equal kinetic-energy densities.

As the blast wave expands, it sweeps up material from the surrounding medium to form an external shock (Mészáros & Rees 1993). Protons captured by the expanding blast wave from the external medium will have total energy $\Gamma m_p c^2$ in the fluid frame, where m_p is the proton mass. The kinetic energy swept into the comoving frame by an uncollimated blast wave at the forward shock per unit time is given by (Blandford & McKee 1976) $dE'/dt' = 4\pi r^2 n_{\rm ext} m_p c^3 \beta\Gamma(\Gamma - 1)$, where the factor of Γ represents the increase of external medium density due to length contraction, the factor $(\Gamma - 1)$ is proportional to the kinetic energy of the swept-up particles, and the factor β is proportional to the rate at which the particles are swept up.

The external shock becomes important when the inertia of the swept-up external matter starts to produce an appreciable slowing of the ejecta. The expanding shell will therefore begin to decelerate when $E = \Gamma M_b c^2 = \Gamma^2 m_p c^2 (4\pi r_{\rm d}^3 n_{\rm ext}/3)$, giving the deceleration radius (Rees & Mészáros 1992, Mészáros & Rees 1993)

$$r_{\rm d} = \left(\frac{3E}{4\pi\Gamma^2 c^2 m_p n_{\rm ext}}\right)^{1/3} \sim 3 \times 10^{16} \left(\frac{E_{52}}{\Gamma_2^2 n_{\rm ext}}\right)^{1/3} \text{ cm}, \tag{7}$$

where $\Gamma \cong E/M_{\rm b}c^2$ is the coasting Lorentz factor, $M_{\rm b}$ is the baryonic mass, $E = 10^{52} E_{52}$ erg is the apparent isotropic energy release, and $n_{\rm ext}$ is the number density of the circumburst medium. This sets a characteristic deceleration length. This deceleration allows slower ejecta to catch up, replenishing and re-energizing the reverse shock and boosting the momentum in the blast wave.

Most treatments employing blast-wave theory to explain the observed afterglow emission from GRBs assume that the radiating particles are electrons. The problem here is that $\sim m_p/m_e \sim 2000$ of the nonthermal particle energy swept into the blast-wave shock is in the form of protons or ions, unless the surroundings are composed primarily of electron-positron pairs. For a radiatively efficient system, physical processes must therefore transfer a large fraction of the swept-up energy to the electron component (Gedalin, Balikhin & Eichler 2008). In most elementary treatments, it is simply assumed that a fraction ϵ_e of the forward-shock power is transferred to the electrons.

The strength of the magnetic field is another major uncertainty. The standard prescription is to assume that the magnetic field's energy density u_B is a fixed fraction ϵ_B of the downstream energy density of the shocked fluid. Hence $u_B = B^2/(8\pi) = 4\epsilon_B n_{\rm ext} m_p c^2 (\Gamma^2 - \Gamma)$ (although see, e.g., Rossi & Rees 2003). It is also generally supposed in simple blast-wave model calculations that some mechanism injects electrons with a power-law distribution between electron Lorentz factors $\gamma_{\rm min} \leq \gamma \leq \gamma_{\rm max}$ downstream of the shock front, where the maximum injection energy is obtained by balancing synchrotron losses and an acceleration rate given in terms of the inverse of the Larmor time scale.

A break is formed in the electron spectrum at cooling electron Lorentz factor $\gamma_{\rm c}$, which is found by balancing the synchrotron loss timescale t'_{sy} with the adiabatic expansion time $t'_{\rm adi} \sim r/(\Gamma c)$ (Sari, Piran & Narayan 1998). For an adiabatic blast wave, $\Gamma \propto t^{-3/8}$, so that $\gamma_{\rm min} \propto t^{-3/8}$ and $\gamma_{\rm c} \propto t^{1/8}$. As a consequence, the accelerated electron minimum random Lorentz factor and the turbulent magnetic field also decrease as inverse power-laws in time (Mészáros & Rees 1993, Rees & Mészáros 1992). This implies that the spectrum softens in time, as the synchrotron peak corresponding to the minimum Lorentz factor and field decreases, leading to the possibility of late long-wavelength emission (Sari, Piran & Narayan 1998).

The relativistic expansion is then gradually slowed down, and the blast wave evolves in a self-similar manner with a power-law light curve. This phase ends when so much mass shares the

energy that the Lorentz factor drops to 1 (Ayal & Piran 2001, Ramirez-Ruiz & MacFadyen 2009). Obviously, this happens when a mass E/c^2 has been swept up. This sets a nonrelativistic mass scale:

$$r_s = \Gamma^{2/3} r_d = \left(\frac{3E}{4\pi m_p c^2 n_{ext}}\right)^{1/3} \sim 10^{18} \left(\frac{E_{52}}{n_{ext}}\right)^{1/3} \text{ cm}. \quad (8)$$

For comparison, the Sedov radius of a supernova that ejects a 10 $M_\odot$ envelope could reach ~5 pc or more.

In GRB sources, with jets that we believe to be highly relativistic, the orientation of the jet axis with respect to our line of sight will strongly affect the source's appearance (Dermer 1995; Dalal, Griest & Pruet 2002; Granot et al. 2002; Ramirez-Ruiz et al. 2005b; Granot 2007), because radiation from jet material will be Doppler beamed in the direction of motion. Attempts to understand the luminosity function of GRBs may have to take into account the statistics of orientation, collimation, and velocity of the jet, as well as the jet's intrinsic radiation properties.

Although our proposed synthesis of GRB physical properties is highly conjectural and far from unique, we hope it will provide a framework for discussing the integrated properties of these objects. We conclude the review by discussing how future observations, experiments, and theoretical studies should enhance our understanding of the physical properties underlying GRBs.

6. PROSPECTS

GRB studies, especially the afterglow-enabled studies of the last ten years, remain a young field. The years ahead are sure to bring astonishing discoveries as the capabilities and experience of observers improve, theorists make more and stronger ties to physical theory, and new and upgraded facilities open vistas. In this section, we summarize the instrumental capabilities and theoretical opportunities for near-term progress in GRB research.

6.1. Facilities

Table 2 summarizes recent and near-future GRB missions. *Swift* (Gehrels et al. 2004) is now the primary mission and has excellent prospects for continued operation, with an orbit that will be stable until at least 2020. *Fermi* and *AGILE*, also in continuing operations, are providing added burst detections with simultaneous high-energy (>100 MeV) coverage that promises to redefine the maximum energies and Lorentz factors that GRB engines are capable of producing.

The Space multi-band Variable Object Monitor (SVOM) mission (Paul et al. 2008), currently under development, promises 4- to 300-keV coverage and *Swift*-like slews that will bring X-ray and optical telescopes to bear on burst positions. The proposed *JANUS* small explorer (Roming 2008) would focus on high-redshift bursts, detecting prompt emission over the 1- to 20-keV band and slewing to observe afterglows with a near-IR telescope (50-cm aperture, 0.7 to 1.7-μm coverage). The proposed large mission *EXIST* has also added fast-response slews and focusing X-ray and near-IR telescopes to its original complement of hard X-ray imaging detectors (Grindlay 2008).

Current and near-future ground-based facilities include a fast-growing array of robotic telescopes primed to respond to burst alerts, ongoing improvements to the instrumentation and capabilities of large-aperture telescopes, a new generation of air-Cerenkov TeV facilities, and the most significant upgrade to a high-sensitivity radio facility in decades—the Expanded Very Large Array (EVLA) initiative.

Rapid follow-up of GRB discoveries is occurring both in space and on the ground; the *Swift* UVOT observes ~80 GRBs per year within 2 min, detecting about half of them. On the ground, fast new telescopes such as ROTSE-III (Akerlof et al. 2003), RAPTOR (Woźniak et al. 2006),

Table 2 Recent and future GRB missions

Mission	Trigger energy range	FOV	Detector area	Other wavelengths	GRB rate (yr^{-1})
BATSE	20 keV–1.9 MeV (LAD)	4π sr	2025 cm^2 per LAD		300
	10 keV–100 MeV (SD)		127 cm^2 per SD		
HETE-2	6–400 keV	3 sr	120 cm^2	X-ray	
Swift	15–150 keV	1.4 sr	5200 cm^2	UV, Optical, X-ray	100 (~10% SGRBs)
AGILE	30 MeV–50 GeV	~3 sr		Hard X-ray	
Fermi	20 MeV–300 GeV (LAT)	>2 sr (LAT)	>8000 cm^2 (LAT)		50
	8 keV to 1 MeV (GBM–LED)	9.5 sr (GBM)	126 cm^2 (GBM–LED)		
	150 keV to 30 MeV (GBM–HED)		126 cm^2 (GBM–HED)		
SVOM	4 keV–300 keV (CXG)	2 sr (CXG)		Optical, X-ray	80
	50 keV–5 MeV (GRM)	89° × 89° (GRM)			
JANUS	1–20 keV	4 sr		Near-IR, X-ray	(high z)
EXIST	5–600 keV (HET)	~3.6 sr (HET)	5.96 m^2 (HET)	Optical, near-IR, X-ray	300

Note: LAD, Large Area Detector; SD, Spectroscopy Detector; LAT, Large Area Telescope; LED, Low Energy Detector; HED, High Energy Detector; CXG, X-ray/gamma-ray Camera; GRM, Gamma-Ray Monitor; GBM, GLAST Burst Monitor; SGRB, short GRB.

Pi-of-the-sky (Burd et al. 2005), and REM (Zerbi et al. 2001) are able to point at GRBs within 10–20 s, and larger facilities like the seven-band GROND (Greiner et al. 2008) respond on 10-min time scales. Ready availability of sensitive CCD and mercury-cadmiun-telluride HgCdTe detectors, combined with rapid-slew mounts and autonomous software systems, should enable further expansion of rapid-response telescopes with more large ($D \gtrsim 2$ m) facilities anticipated in the near future.

GRB-related programs continue to compete successfully for time on premier optical facilities. Large-aperture ($D \gtrsim 6$ m) telescopes provide the spectroscopic observations necessary for GRB redshift measurements. At the Very Large Telescope (VLT), a rapid-response mode has gone further to provide time-sequence observations revealing variable absorption from the host galaxy, and the impending commissioning of the X-Shooter spectrograph (Kaper et al. 2009) will enable full UV to near-IR characterization of afterglow spectra with a single integration. In addition to the Target-of-Opportunity (TOO) opportunities provided by GRB alerts, multiple host-galaxy survey programs are under way.

At radio wavelengths, the workhorse facilities have been the VLA (e.g., Chandra et al. 2008) and WSRT (Westerbork Synthesis Radio Telescope) (e.g., van der Horst et al. 2007), providing data primarily in the range of 1–10 GHz at sensitivities in the 0.2–1.0 mJy range; the EVLA upgrade will improve the sensitivity of that facility to ~10 μJy. Looking ahead, by 2012, the Atacama Large Millimeter Array (ALMA) will be online, operating in the higher-frequency range 90–950 GHz with >100 times the sensitivity of the VLA. The peak in the synchrotron spectrum for a wide range of GRB parameters lies in the ALMA range, making ALMA a potentially powerful future tool for radio observations.

Observations of GRBs at TeV energies can be performed by both narrow-field air Cerenkov facilities and wide-field water Cerenkov detectors; the latter approach, at Milagro, yielded the tentative detection of prompt TeV emission for GRB970417A (Atkins et al. 2003). There has

been no detection to date of prompt or afterglow emission with the air Cerenkov facilities, but significant effort in pursuit of burst alerts is under way at MAGIC, HESS, and VERITAS. The MAGIC dish, in particular, has a rapid-response mode that has provided observations of multiple bursts within a minute of trigger (Albert et al. 2006). Future facilities will seek to lower detection thresholds to $E \sim 100$ GeV, which would provide a significantly expanded horizon within which GRB sources will be visible, rather than attenuated by photon-photon interactions.

In space, the upcoming SM4 promises to revive the HST, providing not only new and resuscitated instruments but also the gyros necessary for flexible and fast-response scheduling. In the future, the capabilities of the *James Webb Space Telescope* will provide an excellent resource for high signal-to-noise observations of highly obscured and high-redshift GRBs.

Within the X-ray band, the *Swift* XRT has redefined all expectations for the characterization of X-ray afterglows and at the same time proved a highly effective facility for refining the multi-arcmin localizations provided by other GRB missions. *Chandra*, *XMM-Newton*, and *Suzaku* continue to be active in GRB observations, and future missions including the Indian ASTROSAT and Japanese/U.S. Astro-H promise added capabilities in the near future. Dramatic improvements will await the next-generation GRB facilities (**Table 2**) or the arrival of the *International X-ray Observatory*.

6.2. Multimessenger Aspects

Given the rapid ongoing expansion of the capabilities of nonelectromagnetic detector facilities, and the extreme luminosity and time-specificity of GRB sources, it will not be long before we either have the first coincident, multi-messenger detection of a GRB, or realize limits on the nonelectromagnetic emissions of GRBs that challenge our current understanding.

The same shocks that are thought to accelerate electrons responsible for the nonthermal γ-rays in GRBs should also accelerate protons, leading ultimately to copious emission of high-energy neutrinos (Waxman 2004b,c, 2006; Dermer & Holmes 2005). The maximum proton energies achievable in GRB shocks are $E_p \sim 10^{20}$ eV, comparable to the highest energies measured with large cosmic-ray ground arrays (Hayashida et al. 1999). For this, the acceleration time must be shorter than both the radiation or adiabatic loss time and the escape time from the acceleration region (Waxman 1995). The accelerated protons can interact with the fireball photons, leading to charged pions, muons, and neutrinos. For internal shocks producing observed 1-MeV photons, this implies $\geq 10^{16}$-eV protons, and neutrinos with $\sim$5% of that energy, $\epsilon_\nu \geq 10^{14}$ eV (Waxman & Bahcall 1997). Another source of copious target photons in the UV is the afterglow reverse shock, for which the resonance condition requires higher-energy protons leading to neutrinos of 10^{17}–10^{19} eV (Waxman & Bahcall 1999). Whereas photon-pion interactions lead to higher-energy neutrinos and provide a direct probe of the shock-proton acceleration as well as of the photon density, inelastic proton-neutron collisions may occur even in the absence of shocks, leading to charged pions and neutrinos (Derishev, Kocharovsky & Kocharovsky 1999) with lower energies than those from photon-pion interactions. The typical neutrino energies are in the $\sim$1–10-GeV range, which could be detectable in coincidence with observed GRBs. This is the province of projects such as IceCube and ANTARES. Neutrino astronomy has the advantage that we can see the Universe up to $\sim$EeV energies. By contrast, the Universe becomes opaque to γ-rays above $\sim$TeV energies through absorption by the IR background.

The last and most challenging frontier is that of gravitational radiation, which is largely unknown territory. A time-integrated luminosity of the order of a solar rest mass ($\sim 10^{54}$ erg) is predicted from progenitor models involving merging compact objects, whereas that from collapsar models is less certain and is expected to be lower by at least one order of magnitude.

Ground-based facilities such as LIGO, TAMA, and VIRGO are currently seeking the first detection of these stellar-scale, high-frequency ($\nu \gtrsim 50$ Hz) sources. The observation of associated gravitational waves would be facilitated if the mergers involve observed short GRB sources; and conversely, it may be possible to strengthen the case for (or against) NS-NS or NS-BH progenitors of short bursts if gravitational waves were detected (or not) in coincidence with some events. The technical challenge of achieving the sensitivities necessary to measure waves from assured sources should not be understated; neither, however, should the potential rewards.

The Enhanced LIGO interferometers will be online in 2009 with the ability to detect NS binary mergers to 20 Mpc. The Advanced LIGO interferometers online in 2014 will extend the distance to 200 Mpc. Short GRBs, if produced by mergers as is thought to be the case, predict a cosmological rate density of >10 Gpc^{-1} year^{-1} with a likely rate of $\sim$300 Gpc^{-1} year^{-1} (O'Shaughnessy et al. 2005, 2008; Nakar 2007b; O'Shaughnessy, Kalogera & Belczynski 2007; O'Shaughnessy, Belczynski & Kalogera 2008a). This translates into an Advanced LIGO detection rate of $\sim$10 year^{-1}. The density estimates include mergers with γ-ray jets not aimed in our direction, so not all LIGO detection would be in coincidence with GRBs. LIGO is already providing useful upper limits, as with GRB070201 described in Section 3.

6.3. Cosmology

One of the frontiers of modern cosmology lies at high redshift, $z \gtrsim 6$, when the first nonlinearities developed into gravitationally bound systems, whose internal evolution gives rise to stars, galaxies, and quasars; and when the light emitted from these first collapsed structures diffuses outward to reionize the Universe. As the (temporarily) brightest source of photons in the cosmos (see **Figure 15**), the demise of these first generations of massive stars in GRB explosions defines the challenge of elucidating the end of the cosmic "dark ages" (Lamb & Reichart 2000, Bromm & Loeb 2002).

Apart from revealing a site of high-redshift star formation, each such high-redshift burst has the potential to help constrain local element abundances in its host galaxy, information that will be impossible to gather by other means until the advent of $D > 20$-m telescopes. Even more exciting, each burst has the potential to reveal the extent of intergalactic reionization at its redshift and along that line of sight (Miralda-Escudé 1998, McQuinn et al. 2008, Mesinger & Furlanetto 2008).

At the highest redshifts, $z \gtrsim 10$, there is growing theoretical evidence that the first luminous objects to form were very massive stars, $M > 100 M_\odot$. Depending on whether these stars retain their high masses until death, and whether a fast-rotating core is a prerequisite to the GRB phenomenon, these Pop III stars might provide the progenitors for the most luminous, highest-redshift GRBs (Heger et al. 2003).

The first GRBs and supernovae may also be important for another reason: They may generate the first cosmic magnetic fields. Mass loss (e.g., via winds) would disperse magnetic flux along with the heavy elements. The ubiquity of heavy elements in the Ly α forest indicates that there has been widespread diffusion from the sites of these early supernovae, and the magnetic flux could have diffused in the same way. This flux, stretched and sheared by bulk motions, could be the "seed" for the later amplification processes that generate the larger-scale fields pervading disc galaxies.

6.4. Theoretical Prospects

What can we expect in the way of matching theoretical progress? This is more difficult to discuss because theory often develops on a shorter time scale than observations and experiments, and

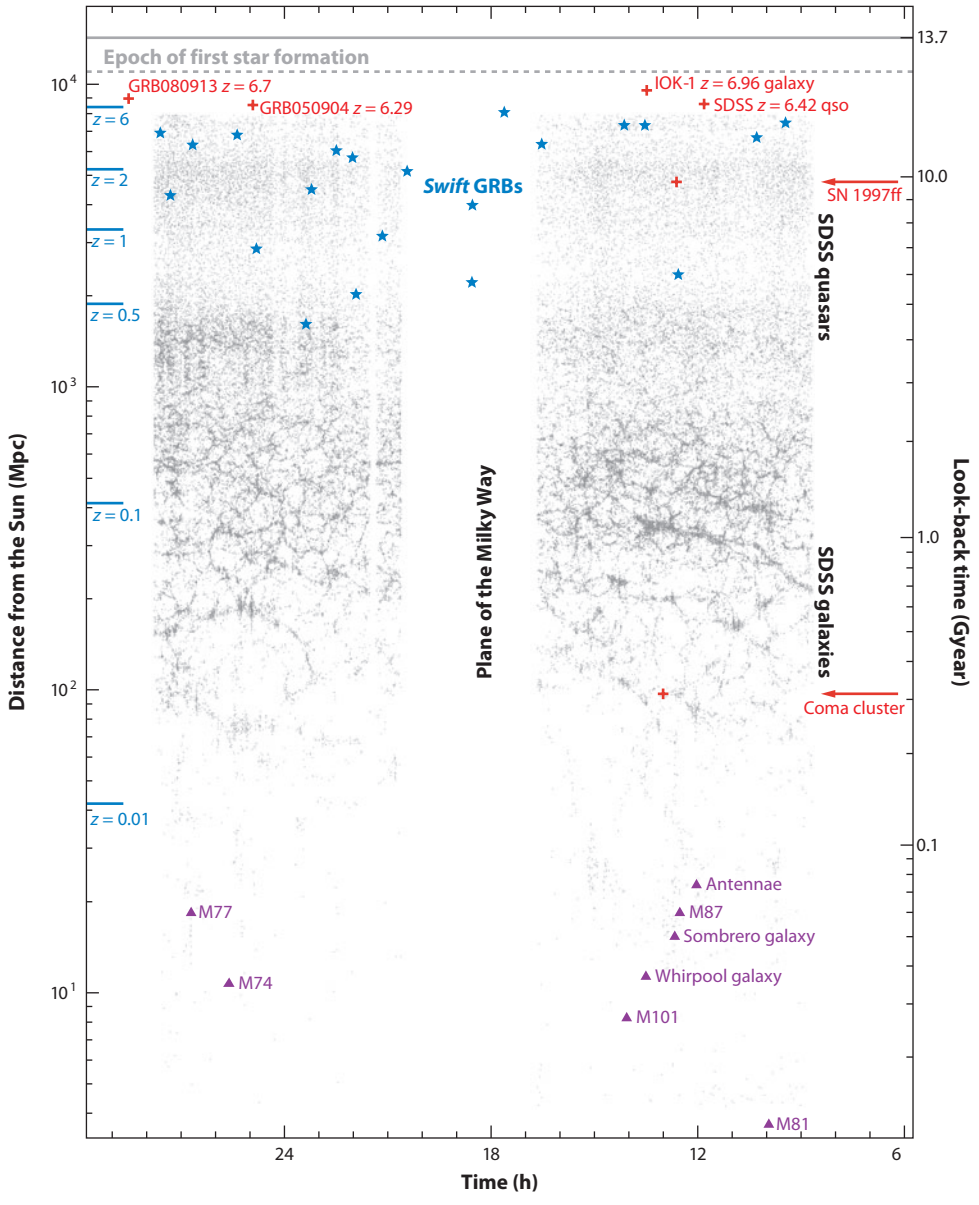

Figure 15

A 360° vista showing the entire sky, with visible structures stretching back in distance, time, and redshift. The most distant light we observe comes from the radiation leftover from the Big Bang: the CMB. As we descend the chart, we find the most distant objects known, followed by a web of Sloan Digital Sky Survey (SDSS) quasars and galaxies. Closer to home, we start to see a collection of familiar "near" galaxies (*purple triangles*). Also marked are all Swift GRBs with known distances (*blue stars*); SN 1997ff, the most distant type Ia supernova at $z = 1.7$; and the archetypal large galaxy cluster, the Coma cluster. The redshift distances of most distant GRBs are comparable to the most distant galaxies and quasars [adapted from Ramirez-Ruiz (2006a)].

so we cannot foresee most future developments. Although some of the features now observed in GRB sources (especially afterglows) were anticipated by theoretical discussions, the recent burst of observational discovery has left theory lagging behind. There are, however, some topics on which we do expect steady work of direct relevance to interpreting observations.

One of the most important is the development and use of hydrodynamical codes for numerical simulation of GRB sources with detailed physics input. Existing two- and three-dimensional codes have already uncovered some gas-dynamical properties of relativistic flows unanticipated by analytical models (McKinney & Blandford 2009), but there are some key questions that they cannot yet address. In particular, higher resolution is needed because even a tiny mass fraction of baryons in the outflow severely limits the maximum attainable Lorentz factor. What is more, jets are undoubtedly susceptible to hydrostatic and hydromagnetic turbulence. We must wait for useful and affordable three-dimensional simulations before we can understand the nonlinear development of instabilities. Well-resolved three-dimensional simulations are becoming increasingly common, and they rarely fail to surprise us. The symmetry breaking involved in transitioning from two to three dimensions is crucial and can lead to qualitatively new phenomena. A particularly important aspect of this would be to link in a self-consistent manner the flow within the accretion disk to that of the outflowing gas, allowing for feedback between the two components. A self-consistent model incorporating inflow and outflow must also explain how some fraction of the material can acquire more than its share of energy (i.e., a high enthalpy or p/ρ).

Particle acceleration and cooling is another problem that seems ripe for a more sophisticated treatment. Everything we know about GRBs is known from photons, and it is widely accepted that these come from particle acceleration in relativistic shocks (Katz, Keshet & Waxman 2007; Ramirez-Ruiz, Nishikawa & Hededal 2007; Medvedev & Spitkovsky 2009; Spitkovsky 2008) or turbulence (Goodman & MacFadyen 2007; Zhang, MacFadyen & Wang 2009; Couch, Milosavljević & Nakar 2008). Because charged particles radiate only when accelerated, one must attempt to deduce from the spectrum how and why the particles are being accelerated, and to identify the macroscopic source driving the microphysical acceleration process.

Collisionless shocks are among the main agents for accelerating ions as well as electrons to high energies whenever sufficient time is available (e.g., Blandford & Eichler 1987, Achterberg et al. 2001). Particles reflected from the shock and from scattering centers behind it in the turbulent compressed region have a good chance of experiencing multiple scattering and acceleration by first-order Fermi acceleration when coming back across the shock into the turbulent upstream region. Second-order or stochastic Fermi acceleration in the broadband turbulence downstream of collisionless shocks will also contribute to acceleration. In addition, ions may be trapped at perpendicular shocks. The trapping is a consequence of the shock and the Lorentz force exerted on the particle by the magnetic and electric fields in the upstream region. With each reflection at the shock, the particles gyrate parallel to the motional electric field, picking up energy and surfing along the shock surface. All these mechanisms are still under investigation, but there is evidence that shocks play a most important role in the acceleration of cosmic rays and other particles to very high energies.

Another topic on which further work seems practicable concerns the kinematics of ultrarelativistic jets (Granot 2007). Although it seems probable that we are using the correct ingredients of special relativity and a collimated outflow, it is equally true that no detailed model yet commands a majority of support. We can still expect some surprises from studies related to the appearance of relativistic shocks in unsteady jets.

The most interesting problem remains, however, the nature of the central engine and the means of extracting power in a useful collimated form. In all observed cases of relativistic jets, the central object is compact, either a NS or BH, and is accreting matter and angular momentum. In

addition, in most systems there is direct or indirect evidence that magnetic fields are present—detected in the synchrotron radiation in galactic and extragalactic radio sources or inferred in collapsing supernova cores from the association of remnants with radio pulsars. This combination of magnetic field and rotation may be very relevant to the production of relativistic jets.

7. CONCLUSIONS

Thanks primarily to the burst discoveries and observations of the *Swift* satellite, the past five years have been tremendously productive ones for GRB research. The identification of short-burst afterglows has confirmed long-held suspicions that GRBs have at least two fundamentally different types of progenitors; subsequent studies of short-burst afterglows and host galaxies have furnished valuable information on the nature of their progenitors and provided clues for next-generation gravity-wave observatories. The discovery of the first three bursts at $z > 6$, before sources reionized most of the hydrogen in the Universe, has proven the value of GRBs as probes of the earliest cosmic epochs and extended GRB observations beyond the redshifts of the most distant known quasars (see **Figure 16**). A flood of prompt burst alerts has fed the queues of more than a dozen dedicated robotic telescopes and prompted fast-response multi-epoch high-resolution spectroscopy from the largest telescopes. Bright GRBs continue to attract the attention of astronomers of all types, with premier facilities across the electromagnetic spectrum poised to respond to the next spectacular event. In the near future, we hope that gravity-wave and high-energy neutrino astronomers will be rewarded for their decades of persistent effort.

The complexity—not to mention sheer volume—of data in the *Swift* era has inevitably raised challenges to the prior interpretation of bursts and their afterglows. However, careful consideration of the biases inherent to the *Swift* mission's observing strategies, along with the large number of

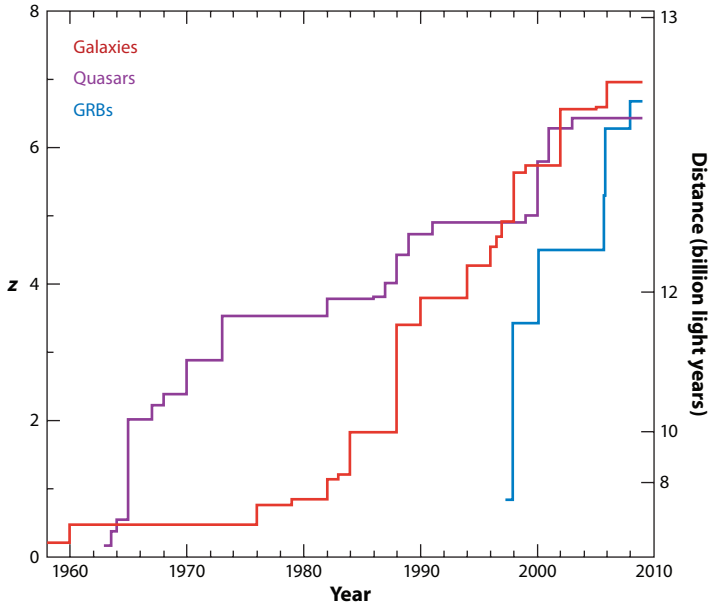

Figure 16

High-z record holders. The history of most distant objects detected in categories of galaxies, quasars, and GRBs. (R. McMahon & N. Tanvir, private communication)

events now available for analysis, is gradually enabling the construction of a single coherent picture via a multidisciplinary approach that addresses data from across the electromagnetic spectrum. It is one of the challenges of contemporary research to infer the underlying physical structure of GRBs in the belief that this is simple, despite the complex character of the observations.

GRBs provide us with an exciting opportunity to study new regimes of physics. As we have described, our rationalization of the principal physical considerations combines some generally accepted features with some more speculative and controversial ingredients. When confronted with observations, it seems to accommodate their gross features but fails to provide a fully predictive theory. What is more valuable, though considerably harder to achieve, is to refine models like the ones advocated here to the point of making quantitative predictions, and to assemble, assess, and interpret observations so as to constrain or refute these theories.

There are good prospects for a continued high rate of discovery. *Swift* is likely to remain operational for many years, and *Fermi* and *AGILE*, now on orbit, are providing new insights at higher energies. Instruments currently being developed or planned have the potential to enable further qualitative advances. GRBs are among the most extraordinary of astronomical phenomena and will, with our present and future capabilities, continue providing a unique window into the extreme reaches of the Universe.

ACKNOWLEDGMENTS

We are indebted to many colleagues for their contributions to this review. We are very grateful to John Cannizzo for his insightful comments and tireless help with editing the manuscript. Several colleagues provided figures and data that we much appreciate. They are Edo Berger, Andy Fruchter, Alexander Kahn, Yuki Kaneko, David Morris, Kim Page, Mario Juric, Jacob Palmatier, Bryan Penprase, J.X. Prochaska, Judy Racusin, Taka Sakamoto, Richard McMahon, and Nial Tanvir. Our views on the topics discussed here have been clarified through discussions with Josh Bloom, Jonathan Granot, William Lee, Peter Mészáros, Udi Nakar, Tsvi Piran, X. Prochaska, Chryssa Kouveliotou, Pawan Kumar, Edo Berger, Alicia Soderberg, Brad Cenko, Dale Frail, Jane Charlton, David Burrows, Doug Cowen, Richard O'Shaughnessy, Kris Belczynski, Kris Stanek, Matthew McQuinn, Hsiao-Wen Chen, Andrew MacFadyen, Sam Oates, Martin J. Rees, Stephan Rosswog, Eli Waxman, Stan Woosley, Chris Fryer, Guillermo Garcia-Segura, Norbert Langer, Sung-Chul Yoon, Dan Kasen, and Annalisa Celotti. We thank J.D. Myers and Rion Parsons for assistance with graphics. Finally, we thank the 200 members of the *Swift* team for the wonderful new findings reported here. This work is partially supported by grants from the National Science Foundation: PHY-0503584 (ER-R), DOE SciDAC: DE-FC02-01ER41176 (ER-R).

LITERATURE CITED

Abbott B, Abbott R, Adhikari R, Ajith P, Allen B, et al. 2008. *Ap. J.* 681:1419
Achterberg A, Gallant YA, Kirk JG, Guthmann AW. 2001. *MNRAS* 328:393
Akerlof C, Balsano R, Barthelemy S, Bloch J, Butterworth P, et al. 1999. *Nature* 398:400
Akerlof CW, Kehoe RL, McKay TA, Rykoff ES, Smith DA, et al. 2003. *Publ. Astron. Soc. Pac.* 115:132
Albert J, Aliu E, Anderhub H, Antoranz P, Armada A, et al. 2006. *Ap. J.* 641:L9
Aloy MA, Janka H-T, Möller E. 2005. *Astron. Astrophys.* 436:273
Aloy MA, Möller E, Ibáñez JM, Martí JM, MacFadyen A. 2000. *Ap. J.* 531:L119
Amati L. 2006. *MNRAS* 372:233
Amati L, Frontera F, Tavani M, in't Zand JJM, Antonelli A, et al. 2002. *Astron. Astrophys.* 390:81
Antonelli LA, Piro L, Vietri M, Costa E, Soffitta P, et al. 2000. *Ap. J.* 545:L39
Atkins R, Benbow W, Berley D, Chen ML, Coyne DG, et al. 2003. *Ap. J.* 583:824

Atwood WB, Abdo AA, Ackermann M, Anderson B, Axelsson M, et al. 2009. *Ap. J.* 697:1071
Ayal S, Piran T. 2001. *Ap. J.* 555:23
Baring MG, Harding AK. 1997. *Ap. J.* 491:663
Barraud C, Olive J-F, Lestrade JP, Atteia J-L, Hurley K, et al. 2003. *Astron. Astrophys.* 400:1021
Barthelmy SD, Barbier LM, Cummings JR, Fenimore EE, Gehrels N, et al. 2005a. *Space Sci. Rev.* 120:143
Barthelmy SD, Cannizzo JK, Gehrels N, Cusumano G, Mangano V, et al. 2005b. *Ap. J.* 635:L133
Barthelmy SD, Chincarini G, Burrows DN, Gehrels N, Covino S, et al. 2005c. *Nature* 438:994
Belczynski K, Bulik T, Rudak B. 2002. *Ap. J.* 571:394
Belczynski K, Perna R, Bulik T, Kalogera V, Ivanova N, et al. 2006. *Ap. J.* 648:1110
Beloborodov AM. 2003. *Ap. J.* 585:L19
Berger E. 2009. *Ap. J.* 690:231
Berger E, Fox DB, Kulkarni SR, Frail DA, Djorgovski SG. 2007a. *Ap. J.* 660:504
Berger E, Fox DB, Price PA, Nakar E, Gal-Yam A, et al. 2007b. *Ap. J.* 664:1000
Berger E, Penprase BE, Fox DB, Kulkarni SR, Hill G, et al. 2005a. (astro-ph/0512280)
Berger E, Price PA, Cenko SB, Gal-Yam A, Soderberg AM, et al. 2005b. *Nature* 438:988
Bhat PN, Fishman GJ, Meegan CA, Wilson RB, Brock MN, et al. 1992. *Nature* 359:217
Blake CH, Bloom JS, Starr DL, Falco EE, Skrutskie M, et al. 2005. *Nature* 435:181
Blandford R, Eichler D. 1987. *Phys. Fluids* 154:1
Blandford RD, McKee CF. 1976. *Phys. Fluids* 19:1130
Blandford RD, Payne DG. 1982. *MNRAS* 199:883
Blandford RD, Znajek RL. 1977. *MNRAS* 179:433
Bloom JS, Frail DA, Kulkarni SR. 2003. *Ap. J.* 594:674
Bloom JS, Frail DA, Sari R. 2001. *Ap. J.* 121:2879
Bloom JS, Kulkarni SR, Djorgovski SG. 2002. *Ap. J.* 123:1111
Bloom JS, Perley DA, Chen H-W, Butler N, Prochaska JX, et al. 2007. *Ap. J.* 654:878
Bloom JS, Perley DA, Li W, Butler NR, Miller AA, et al. 2009. *Ap. J.* 691:723
Bloom JS, Prochaska JX. 2006. In *Gamma-Ray Bursts in the Swift Era*, Vol. 836 of Am. Inst. Phys. Conf. Ser., ed. SS Holt, N Gehrels, JA Nousek, p. 473. Am. Inst. Phys.: Melville, NY
Bloom JS, Prochaska JX, Pooley D, Blake CH, Foley RJ, et al. 2006. *Ap. J.* 638:354
Blustin AJ, Band D, Barthelmy S, Boyd P, Capalbi M, et al. 2006. *Ap. J.* 637:901
Boër M, Atteia JL, Damerdji Y, Gendre B, Klotz A, Stratta G. 2006. *Ap. J.* 638:L71
Bromm V, Loeb A. 2002. *Ap. J.* 575:111
Bucciantini N, Quataert E, Arons J, Metzger BD, Thompson TA. 2008. *MNRAS* 383:L25
Burd A, Cwiok M, Czyrkowski H, Dabrowski R, Dominik W, et al. 2005. *New Astron.* 10:409
Burrows DN, Hill JE, Nousek JA, Kennea JA, Wells A, et al. 2005a. *Space Sci. Rev.* 120:165
Burrows DN, Romano P, Falcone A, Kobayashi S, Zhang B, et al. 2005b. *Science* 309:1833
Castro-Tirado AJ, de Ugarte Postigo A, Gorosabel J, Fathkullin T, Sokolov V, et al. 2005. *Astron. Astrophys.* 439:L15
Cenko SB, Kasliwal M, Harrison FA, Pal'shin V, Frail DA, et al. 2009. *Ap. J. L.* Submitted (astro-ph/0802.0874)
Cenko SB, Kasliwal M, Harrison FA, Pal'shin V, Frail DA, et al. 2006. *Ap. J.* 652:490
Chandra P, Cenko SB, Frail DA, Chevalier RA, Macquart J-P, et al. 2008. *Ap. J.* 683:924
Chary R, Berger E, Cowie L. 2007. *Ap. J.* 671:272
Chen H-W, Perley DA, Pollack LK, Prochaska JX, Bloom JS, et al. 2009. *Ap. J.* 691:152
Chen H-W, Prochaska JX, Bloom JS, Thompson IB. 2005. *Ap. J.* 634:L25
Chen H-W, Prochaska JX, Ramirez-Ruiz E, Bloom JS, Dessauges-Zavadsky M, et al. 2007. *Ap. J.* 663:420
Chen W-X, Beloborodov AM. 2007. *Ap. J.* 657:383
Chincarini G, Moretti A, Romano P, Falcone AD, Morris D, et al. 2007. *Ap. J.* 671:1903
Christensen L, Hjorth J, Gorosabel J. 2004. *Astron. Astrophys.* 425:913
Cline TL, Desai UD. 1974. *NASA STI/Recon.Tech. Rep. N* 75:11888
Connaughton V. 2002. *Ap. J.* 567:1028
Conselice CJ, Vreeswijk PM, Fruchter AS, Levan A, Kouveliotou C, et al. 2005. *Ap. J.* 633:29
Couch SM, Milosavljević M, Nakar E. 2008. *Ap. J.* 688:462
Courty S, Björnsson G, Gudmundsson EH. 2004. *MNRAS* 354:581

Courty S, Björnsson G, Gudmundsson EH. 2007. *MNRAS* 376:1375
Covino S, Malesani D, Israel GL, D'Avanzo P, Antonelli LA, et al. 2006. *Astron. Astrophys.* 447:L5
Cusumano G, Mangano V, Chincarini G, Panaitescu A, Burrows DN, et al. 2006. *Nature* 440:164
Dai X, Garnavich PM, Prieto JL, Stanek KZ, Kochanek CS, et al. 2008. *Ap. J.* 682:L77
Dai X, Halpern JP, Morgan ND, Armstrong E, Mirabal N, et al. 2007. *Ap. J.* 658:509
Dalal N, Griest K, Pruet J. 2002. *Ap. J.* 564:209
D'Avanzo P, Malesani D, Covino S, Piranomonte S, Grazian A, et al. 2009. *Astron. Astrophys.* 498:711–21
D'Elia V, Fiore F, Perna R, Krongold Y, Coviny S, et al. 2009. *Ap. J.* 694:332
Della Valle M, Chincarini G, Panagia N, Tagliaferri G, Malesani D, et al. 2006a. *Nature* 444:1050
Della Valle M, Chincarini G, Panagia N, Tagliaferri G, Malesani D, et al. 2006b. *Nature* 444:1050
Derishev EV, Kocharovsky VV, Kocharovsky Vl V. 1999. *Ap. J.* 521:640
Dermer CD. 1995. *Ap. J.* 446:L63
Dermer CD, Holmes JM. 2005. *Ap. J.* 628:L21
Dessart L, Burrows A, Livne E, Ott CD. 2008. *Ap. J.* 673:L43
Dessart L, Ott CD, Burrows A, Rosswog S, Livne E. 2009. *Ap. J.* 690:1681
Di Matteo T, Perna R, Narayan R. 2002. *Ap. J.* 579:706
Duncan RC, Thompson C. 1992. *Ap. J.* 392:L9
Evans PA, Beardmore AP, Page KL, Osborne JP, O'Brien PT, et al. 2009. *MNRAS* Submitted (astro-ph/0812.3662)
Evans PA, Beardmore AP, Page KL, Tyler LG, Osborne JP, et al. 2007. *Astron. Astrophys.* 469:379
Falcone AD, Morris D, Racusin J, Chincarini G, Moretti A, et al. 2007. *Ap. J.* 671:1921
Fenimore EE, Epstein RI, Ho C. 1993. *Astron. Astrophys. S* 97:59
Fenimore EE, Klebesadel RW, Laros JG. 1996. *Ap. J.* 460:964
Fenimore EE, Madras CD, Nayakshin S. 1996. *Ap. J.* 473:998
Fenimore EE, Palmer D, Galassi M, Tavenner T, Barthelmy S, et al. 2003. In *Gamma-Ray Burst and Afterglow Astronomy 2001: A Workshop Celebrating the First Year of the HETE Mission*, Vol. 662 of Am. Inst. Phys. Conf. Ser., ed. GR Ricker, RK Vanderspek, p. 491. Am. Inst. Phys.: Melville, NY
Fenimore EE, Ramirez-Ruiz E. 2000. (astro-ph/0004176)
Firmani C, Ghisellini G, Avila-Reese V, Ghirlanda G. 2006. *MNRAS* 370:185
Foley RJ, Bloom JS, Prochaska JX, Illingworth GD, Holden BP, et al. 2005. *GRB Coord. Netw.* 4409:1
Fox AJ, Ledoux C, Vreeswijk PM, Smette A, Jaunsen AO. 2008. *Astron. Astrophys.* 491:189
Fox DB, Frail DA, Price PA, Kulkarni SR, Berger E, et al. 2005. *Nature* 437:845
Fox DB, Roming PWA. 2007. *R. Soc. Lond. Philos. Trans. Ser. A* 365:1293
Frail DA, Cameron PB, Kasliwal M, Nakar E, Price PA, et al. 2006. *Ap. J.* 646:L99
Frail DA, Kulkarni SR, Nicastro L, Feroci M, Taylor GB. 1997. *Nature* 389:261
Frail DA, Kulkarni SR, Sari R, Djorgovski SG, Bloom JS, et al. 2001. *Ap. J.* 562:L55
Freedman DL, Waxman E. 2001. *Ap. J.* 547:922
Fruchter AS, Levan AJ, Strolger L, Vreeswijk PM, Thorsett SE, et al. 2006. *Nature* 441:463
Fryer CL, Woosley SE, Hartmann DH. 1999. *Ap. J.* 526:152
Fynbo JPU, Jakobsson P, Möller P, Hjorth J, Thomsen B, et al. 2003. *Astron. Astrophys.* 406:L63
Fynbo JPU, Prochaska JX, Sommer-Larsen J, Dessauges-Zavadsky M, Møller P. 2008. *Ap. J.* 683:321
Fynbo JPU, Starling RLC, Ledoux C, Wiersema K, Thöne CC, et al. 2006a. *Astron. Astrophys.* 451:L47
Fynbo JPU, Watson D, Thöne CC, Sollerman J, Bloom JS, et al. 2006b. *Nature* 444:1047
Gaensler BM, Kouveliotou C, Gelfand JD, Taylor GB, Eichler D, et al. 2005. *Nature* 434:1104
Gal-Yam A, Fox DB, Price PA, Ofek EO, Davis MR, et al. 2006. *Nature* 444:1053
Gal-Yam A, Nakar E, Ofek EO, Cenko SB, Kulkarni SR, et al. 2008. *Ap. J.* 686:408
Galama TJ, Vreeswijk PM, van Paradijs J, Kouveliotou C, Augusteijn T, et al. 1998. *Nature* 395:670
Gedalin M, Balikhin MA, Eichler D. 2008. *Phys. Rev. E* 77(2):026403
Gehrels N, Barthelmy SD, Burrows DN, Cannizzo JK, Chincarini G, et al. 2008. *Ap. J.* 689:1161
Gehrels N, Chincarini G, Giommi P, Mason KO, Nousek JA, et al. 2004. *Ap. J.* 611:1005
Gehrels N, Norris JP, Barthelmy SD, Granot J, Kaneko Y, et al. 2006. *Nature* 444:1044
Gehrels N, Sarazin CL, O'Brien PT, Zhang B, Barbier L, et al. 2005. *Nature* 437:851
Ghirlanda G, Ghisellini G, Lazzati D. 2004. *Ap. J.* 616:331

Giannios D, Spruit HC. 2007. *Astron. Astrophys.* 469:1
Gold T. 1968. *Nature* 218:731
Goodman J. 1986. *Ap. J.* 308:L47
Goodman J, Dar A, Nussinov S. 1987. *Ap. J.* 314:L7
Goodman J, MacFadyen AI. 2007. (astro-ph/0706.1818)
Gou L-J, Fox DB, Mészáros P. 2007. *Ap. J.* 668:1083
Granot J. 2007. *Rev. Mex. Astron. Astrofís. Conf. Ser.* 27:140
Granot J. 2008. In *Proc. 070228: The Next Decade of Gamma-Ray Burst Afterglows, Amsterdam, March 19–23, 2007*, ed. RAMJ Wijers, L Kaper, HJ van Eerten. Amsterdam: Elsevier. (astro-ph/0811.1657)
Granot J, Cohen-Tanugi J, do Couto e Silva E. 2008. *Ap. J.* 677:92
Granot J, Kumar P. 2006. *MNRAS* 366:L13
Granot J, Panaitescu A, Kumar P, Woosley SE. 2002. *Ap. J.* 570:L61
Granot J, Ramirez-Ruiz E. 2004. *Ap. J.* 609:L9
Granot J, Ramirez-Ruiz E, Loeb A. 2005a. *Ap. J.* 618:413
Granot J, Ramirez-Ruiz E, Perna R. 2005b. *Ap. J.* 630:1003
Greiner J, Bornemann W, Clemens C, Deuter M, Hasinger G, et al. 2008. *Publ. Astron. Soc. Pac.* 120:405
Grindlay J. 2008. See Holt & White 2008, p. 1084
Grupe D, Gronwall C, Wang X-Y, Roming PWA, Cummings J, et al. 2007. *Ap. J.* 662:443
Guetta D, Granot J, Begelman MC. 2005. *Ap. J.* 622:482
Guetta D, Piran T. 2006. *Astron. Astrophys.* 453:823
Guetta D, Piran T. 2007. *J. Cosmol. Astro-Particle Phys.* 7:3
Guilbert PW, Fabian AC, Rees MJ. 1983. *MNRAS* 205:593
Haislip JB, Nysewander MC, Reichart DE, Levan A, Tanvir N, et al. 2006. *Nature* 440:181
Hayashida N, Nagano M, Nishikawa D, Ohoka H, Sakaki N, et al. 1999. *Astroparticle Phys.* 10:303
Heger A, Fryer CL, Woosley SE, Langer N, Hartmann DH. 2003. *Ap. J.* 591:288
Heise J, in't Zand J, Kippen RM, Woods PM. 2001. In *Gamma-ray Bursts in the Afterglow Era*, ed. E Costa, F Frontera, J Hjorth, p. 16. New York, NY: Springer
Hjorth J, Sollerman J, Gorosabel J, Granot J, Klose S, et al. 2005a. *Ap. J.* 630:L117
Hjorth J, Sollerman J, Møller P, Fynbo JPU, Woosley SE, et al. 2003. *Nature* 423:847
Hjorth J, Watson D, Fynbo JPU, Price PA, Jensen BL, et al. 2005b. *Nature* 437:859
Holt SS, White N, eds. 2008. *Comm. Space Res. (COSPAR) Plenary Meet.*, Vol. 37. Amsterdam: Elsevier
Horack JM, Koshut TM, Mallozzi RS, Storey SD, Emslie AG. 1994. *Ap. J.* 429:319
Houck JC, Chevalier RA. 1991. *Ap. J.* 376:234
Hurkett CP, Vaughan S, Osborne JP, O'Brien PT, Page KL, et al. 2008. *Ap. J.* 679:587
Hurley K, Boggs SE, Smith DM, Duncan RC, Lin R, et al. 2005. *Nature* 434:1098
Hurley K, Cline T, Mazets E, Barthelmy S, Butterworth P, et al. 1999. *Nature* 397:41
Izzard RG, Ramirez-Ruiz E, Tout CA. 2004. *MNRAS* 348:1215
Jakobsson P, Levan A, Fynbo JPU, Priddey R, Hjorth J, et al. 2006. *Astron. Astrophys.* 447:897
Kaneko Y, González MM, Preece RD, Dingus BL, Briggs MS. 2008. *Ap. J.* 677:1168
Kaneko Y, Ramirez-Ruiz E, Granot J, Kouveliotou C, Woosley SE, et al. 2007. *Ap. J.* 654:385
Kann DA, Klose S, Zhang B, Malesani D, Nakar E, et al. 2007. (astro-ph/0712.2186)
Kaper L, D'Odorico S, Hammer F, Pallavicini R, Kjaergaard Rasmussen P, et al. 2009. In *Science with the VLT in the ELT Era*, ed. A Moorwood, p 319. New York, NY: Springer
Katz B, Keshet U, Waxman E. 2007. *Ap. J.* 655:375
Katz JI. 1994. *Ap. J.* 422:248
Katz JI, Canel LM. 1996. *Ap. J.* 471:915
Kawabata KS, Deng J, Wang L, Mazzali P, Nomoto K, et al. 2003. *Ap. J.* 593:L19
Kawai N, Kosugi G, Aoki K, Yamada T, Totani T, et al. 2006. *Nature* 440:184
Kehoe R, Akerlof C, Balsano R, Barthelmy S, Bloch J, et al. 2001. *Ap. J.* 554:L159
Kippen RM, Woods PM, Heise J, in't Zand JJM, Briggs MS, et al. 2003. In *Gamma-Ray Burst and Afterglow Astronomy 2001: A Workshop Celebrating the First Year of the HETE Mission, AIP Conf. Proc. 662*, ed. GR Ricker, RK Vanderspek, p. 244. Melville, NY: Am. Inst. Phys.
Kistler MD, Yüksel H, Beacom JF, Stanek KZ. 2008. *Ap. J.* 673:L119

Klebesadel RW, Strong IB, Olson RA. 1973. *Ap. J.* 182:L85
Klotz A, Gendre B, Stratta G, Atteia JL, Boër M, et al. 2006. *Astron. Astrophys.* 451:L39
Kluzniak W, Lee WH. 1998. *Ap. J.* 494:L53
Kobayashi S, Ryde F, MacFadyen A. 2002. *Ap. J.* 577:302
Kobulnicky HA, Kewley LJ. 2004. *Ap. J.* 617:240
Kocevski D, Butler N. 2008. *Ap. J.* 680:531
Kouveliotou C, Meegan CA, Fishman GJ, Bhat NP, Briggs MS, et al. 1993. *Ap. J.* 413:L101
Kuiper L, Hermsen W, Cusumano G, Diehl R, Schönfelder V, et al. 2001. *Astron. Astrophys.* 378:918
Kumar P, McMahon E. 2008. *MNRAS* 384:33
Kumar P, Narayan R. 2009. *MNRAS* 395:472
Kumar P, Narayan R, Johnson JL. 2008. *MNRAS* 388:1729
Kumar P, Panaitescu A. 2000. *Ap. J.* 541:L51
Kumar P, Panaitescu A. 2008. *MNRAS* 391:L19
Lamb DQ, Reichart DE. 2000. *Ap. J.* 536:1
Lamb DQ, Ricker GR, Atteia J-L, Barraud C, Boer M, et al. 2004. *New Astron. Rev.* 48:423
Lazzati D, Ramirez-Ruiz E, Ghisellini G. 2001. *Astron. Astrophys.* 379:L39
Le T, Dermer CD. 2007. *Ap. J.* 661:394
Le Floc'h E, Charmandaris V, Forrest WJ, Mirabel IF, Armus L, et al. 2006. *Ap. J.* 642:636
Le Floc'h E, Duc P-A, Mirabel IF, Sanders DB, Bosch G, et al. 2003. *Astron. Astrophys.* 400:499
Lee WH, Ramirez-Ruiz E. 2006. *Ap. J.* 641:961
Lee WH, Ramirez-Ruiz E. 2007. *New J. Phys.* 9:17
Lee WH, Ramirez-Ruiz E, Granot J. 2005. *Ap. J.* 630:L165
Lee WH, Ramirez-Ruiz E, Page D. 2004. *Ap. J.* 608:L5
Lee WH, Ramirez-Ruiz E, Page D. 2005. *Ap. J.* 632:421
Levinson A, Eichler D. 2000. *Phys. Rev. Lett.* 85:236
Lithwick Y, Sari R. 2001. *Ap. J.* 555:540
Lloyd-Ronning NM, Ramirez-Ruiz E. 2002. *Ap. J.* 576:101
Lopez-Camara D, Lee WH, Ramirez-Ruiz E. 2009. *Ap. J.* 692:804
Lyutikov M, Blandford R. 2003. (astro-ph/0312347)
MacFadyen AI, Woosley SE. 1999. *Ap. J.* 524:262
MacFadyen AI, Woosley SE, Heger A. 2001. *Ap. J.* 550:410
Matheson T, Garnavich PM, Stanek KZ, Bersier D, Holland ST, et al. 2003. *Ap. J.* 599:394
Matsuoka M, Kawai N, Yoshida A, Tamagawa T, Torii K, et al. 2004. *Baltic Astron.* 13:201
Matzner CD. 2003. *MNRAS* 345:575
Mazets EP, Aptekar RL, Cline TL, Frederiks DD, Goldsten JO, et al. 2008. *Ap. J.* 680:545
Mazets EP, Golenetskii SV, Ilyinskii VN, Panov VN, Aptekar RL, et al. 1981. *Ap. Space Sci.* 80:85
McConnell ML, Zdziarski AA, Bennett K, Bloemen H, Collmar W, et al. 2002. *Ap. J.* 572:984
McKinney JC. 2006. *MNRAS* 368:1561
McKinney JC, Blandford RD. 2009. *MNRAS* 394:L126
McQuinn M, Lidz A, Zaldarriaga M, Hernquist L, Dutta S. 2008. *MNRAS* 388:1101
Medvedev MV, Spitkovsky A. 2009. *Ap. J.* Submitted (astro-ph/0810.4014)
Mesinger A, Furlanetto SR. 2008. *MNRAS* 385:1348
Mészáros P. 2002. *Annu. Rev. Astron. Astrophys.* 40:137
Mészáros P, Ramirez-Ruiz E, Rees MJ, Zhang B. 2002. *Ap. J.* 578:812
Mészáros P, Rees MJ. 1993. *Ap. J.* 405:278
Mészáros P, Rees MJ. 1997. *Ap. J.* 476:232
Mészáros P, Rees MJ. 1997. *Ap. J.* 482:L29
Mészáros P, Rees MJ. 1999. *MNRAS* 306:L39
Mészáros P, Rees MJ. 2000. *Ap. J.* 530:292
Mészáros P, Rees MJ. 2001. *Ap. J.* 556:L37
Mészáros P, Rees MJ, Papathanassiou H. 1994. *Ap. J.* 432:181
Mészáros P, Waxman E. 2001. *Phys. Rev. Lett.* 87(17):171102
Metzger BD, Piro AL, Quataert E. 2008. *MNRAS* 390:781

Metzger BD, Thompson TA, Quataert E. 2007. *Ap. J.* 659:561
Metzger MR, Djorgovski SG, Kulkarni SR, Steidel CC, Adelberger KL, et al. 1997. *Nature* 387:878
Mirabal N, Halpern JP, Chornock R, Filippenko AV, Terndrup DM, et al. 2003. *Ap. J.* 595:935
Miralda-Escudé J. 1998. *Ap. J.* 501:15
Mochkovitch R, Hernanz M, Isern J, Martin X. 1993. *Nature* 361:236
Modjaz M, Kewley L, Kirshner RP, Stanek KZ, Challis P, et al. 2008. *AJ* 135:1136
Molinari E, Vergani SD, Malesani D, Covino S, D'Avanzo P, et al. 2007. *Astron. Astrophys.* 469:L13
Möller P, Fynbo JPU, Hjorth J, Thomsen B, Egholm MP, et al. 2002. *Astron. Astrophys.* 396:L21
Morsony BJ, Lazzati D, Begelman MC. 2007. *Ap. J.* 665:569
Nakar E. 2007a. *Phys. Fluids* 442:166
Nakar E. 2007b. *Adv. Space Res.* 40:1224
Nakar E, Gal-Yam A, Fox DB. 2006. *Ap. J.* 650:281
Nakar E, Gal-Yam A, Piran T, Fox DB. 2006. *Ap. J.* 640:849
Narayan R, Paczyński B, Piran T. 1992. *Ap. J.* 395:L83
Narayan R, Piran T, Kumar P. 2001. *Ap. J.* 557:949
Norris JP, Bonnell JT. 2006. *Ap. J.* 643:266
Norris JP, Cline TL, Desai UD, Teegarden BJ. 1984. *Nature* 308:434
Norris JP, Gehrels N. 2008. In *American Institute of Physics Conference Series*, ed. M Galassi, D Palmer, E Fenimore, 1000:280. Melville, NY: Am. Inst. Phys.
Norris JP, Nemiroff RJ, Bonnell JT, Scargle JD, Kouveliotou C, et al. 1996. *Ap. J.* 459:393
Nousek JA, Kouveliotou C, Grupe D, Page KL, Granot J, et al. 2006. *Ap. J.* 642:389
Nysewander M, Fruchter AS, Pe'er A. 2009. *Ap. J.* Submitted (astro-ph/0806.3607)
Oates SR, Page MJ, Schady P, de Pasquale M, Koch TS et al. 2009. *MNRAS* 395:490
O'Brien PT, Willingale R, Osborne J, Goad MR, Page KL, et al. 2006. *Ap. J.* 647:1213
Ofek EO, Cenko SB, Gal-Yam A, Fox DB, Nakar E, et al. 2007. *Ap. J.* 662:1129
Oren Y, Nakar E, Piran T. 2004. *MNRAS* 353:L35
O'Shaughnessy R, Belczynski K, Kalogera V. 2008. *Ap. J.* 675:566
O'Shaughnessy R, Kalogera V, Belczynski K. 2007. *Ap. J.* 667:1048
O'Shaughnessy R, Kim C, Fragos T, Kalogera V, Belczynski K. 2005. *Ap. J.* 633:1076
O'Shaughnessy R, Kim C, Kalogera V, Belczynski K. 2008. *Ap. J.* 672:479
Pacini F. 1967. *Nature* 216:567
Paczyński B. 1986. *Ap. J.* 308:L43
Paczyński B. 1990. *Ap. J.* 363:218
Paczyński B. 1998. *Ap. J.* 494:L45
Paczyński B, Xu G. 1994. *Ap. J.* 427:708
Palmer DM, Barthelmy S, Gehrels N, Kippen RM, Cayton T, et al. 2005. *Nature* 434:1107
Panaitescu A, Mészáros P, Burrows D, Nousek J, Gehrels N, et al. 2006. *MNRAS* 369:2059
Paul J, Wei J, Zhang S, Basa S. 2008. See Holt & White 2008, p. 2368
Pe'er A, Mészáros P, Rees MJ. 2006. *Ap. J.* 642:995
Penprase BE, Berger E, Fox DB, Kulkarni SR, Kadish S, et al. 2006. *Ap. J.* 646:358
Perna R, Armitage PJ, Zhang B. 2006. *Ap. J.* 636:L29
Pian E, Mazzali PA, Masetti N, Ferrero P, Klose S, et al. 2006. *Nature* 442:1011
Pihlström YM, Taylor GB, Granot J, Doeleman S. 2007. *Ap. J.* 664:411
Piran T, Kumar P, Panaitescu A, Piro L. 2001. *Ap. J.* 560:L167
Piran T, Sari R, Zou Y-C. 2009. *MNRAS* 383:1107
Piran T, Shemi A. 1993. *Ap. J.* 403:L67
Piro L, Costa E, Feroci M, Frontera F, Amati L, et al. 1999. *Ap. J.* 514:L73
Piro L, Garmire G, Garcia M, Stratta G, Costa E, et al. 2000. *Science* 290:955
Podsiadlowski P, Mazzali PA, Nomoto K, Lazzati D, Cappellaro E. 2004. *Ap. J.* 607:L17
Porciani C, Madau P. 2001. *Ap. J.* 548:522
Porciani C, Viel M, Lilly SJ. 2007. *Ap. J.* 659:218
Preece RD, Briggs MS, Mallozzi RS, Pendleton GN, Paciesas WS, et al. 2000. *ApJS* 126:19
Price DJ, Rosswog S. 2006. *Science* 312:719

Price PA, Songaila A, Cowie LL, Bell Burnell J, Berger E, et al. 2007. *Ap. J.* 663:L57
Prochaska JX, Chen H-W, Bloom JS. 2006. *Ap. J.* 648:95
Prochaska JX, Chen H-W, Bloom JS, Dessauges-Zavadsky M, O'Meara JM, et al. 2007. *ApJS* 168:231
Prochaska JX, Dessauges-Zavadsky M, Ramirez-Ruiz E, Chen H-W. 2008. *Ap. J.* 685:344
Prochaska JX, Sheffer Y, Perley DA, Bloom JS, Lopez LA, et al. 2009. *Ap. J.* 691:L27
Prochter GE, Prochaska JX, Chen H-W, Bloom JS, Dessauges-Zavadsky M, et al. 2006. *Ap. J.* 648:L93
Proga D, MacFadyen AI, Armitage PJ, Begelman MC. 2003. *Ap. J.* 599:L5
Proga D, Zhang B. 2006. *MNRAS* 370:L61
Qian Y-Z., Woosley SE. 1996. *Ap. J.* 471:331
Quimby RM, Rykoff ES, Yost SA, Aharonian F, Akerlof CW, et al. 2006. *Ap. J.* 640:402
Racusin JL, Karpov SV, Sokolowski M, Granot J, Wu XF, et al. 2008. *Nature* 455:183
Racusin JL, Liang EW, Burrows DN, Falcone A, Sakamoto T, et al. 2009. *Ap. J.* Submitted (arXiv 0812.4780)
Ramirez-Ruiz E. 2005. *MNRAS* 363:L61
Ramirez-Ruiz E. 2006a. *Nature* 440:154
Ramirez-Ruiz E. 2006b. *Nuovo Cim. B* 121:1261
Ramirez-Ruiz E, Celotti A, Rees MJ. 2002a. *MNRAS* 337:1349
Ramirez-Ruiz E, Fenimore EE. 2000. *Ap. J.* 539:712
Ramirez-Ruiz E, García-Segura G, Salmonson JD, Pérez-Rendón B. 2005a. *Ap. J.* 631:435
Ramirez-Ruiz E, Granot J, Kouveliotou C, Woosley SE, Patel SK, Mazzali PA. 2005b. *Ap. J.* 625:L91
Ramirez-Ruiz E, Lazzati D, Blain AW. 2002b. *Ap. J.* 565:L9
Ramirez-Ruiz E, Lloyd-Ronning NM. 2002. *New Astron.* 7:197
Ramirez-Ruiz E, MacFadyen AI. 2009. *Ap. J.* Submitted (astro-ph/0808.3448)
Ramirez-Ruiz E, MacFadyen AI, Lazzati D. 2002c. *MNRAS* 331:197
Ramirez-Ruiz E, Nishikawa K-I, Hededal CB. 2007. *Ap. J.* 671:1877
Rees MJ, Mészáros P. 1992. *MNRAS* 258:41P
Rees MJ, Mészáros P. 1994. *Ap. J.* 430:L93
Reeves JN, Watson D, Osborne JP, Pounds KA, O'Brien PT, et al. 2002. *Nature* 416:512
Reichart DE, Lamb DQ, Fenimore EE, Ramirez-Ruiz E, Cline TL, Hurley K. 2001. *Ap. J.* 552:57
Rhoads JE. 1999. *Ap. J.* 525:737
Romano P, Campana S, Mignani RP, Moretti A, Mottini M, et al. 2008. *VizieR Online Data Catalog* 348:81221
Roming P. 2008. See Holt & White 2008, p. 2645
Roming PWA, Kennedy TE, Mason KO, Nousek JA, Ahr L, et al. 2005. *Space Sci. Rev.* 120:95
Roming PWA, Koch TS, Oates SR, Porterfield BL, Vanden Berk DE, et al. 2009. *Ap. J.* 690:163
Rossi E, Rees MJ. 2003. *MNRAS* 339:881
Rosswog S, Liebendörfer M. 2003. *MNRAS* 342:673
Rosswog S, Ramirez-Ruiz E. 2002. *MNRAS* 336:L7
Rosswog S, Ramirez-Ruiz E, Davies MB. 2003. *MNRAS* 345:1077
Rosswog S, Speith R, Wynn GA. 2004. *MNRAS* 351:1121
Ruffert M, Janka H-T, Takahashi K, Schaefer G. 1997. *Astron. Astrophys.* 319:122
Ryde F, Pe'er A. 2009. *Ap. J.* Submitted (astro-ph/0811.4135)
Rykoff ES, Aharonian F, Akerlof CW, Alatalo K, Ashley MCB, et al. 2005. *Ap. J.* 631:1032
Rykoff ES, Mangano V, Yost SA, Sari R, Aharonian F, et al. 2006. *Ap. J.* 638:L5
Rykoff ES, Smith DA, Price PA, Akerlof CW, Ashley MCB, et al. 2004. *Ap. J.* 601:1013
Rykoff ES, Yost SA, Krimm HA, Aharonian F, Akerlof CW, et al. 2005. *Ap. J.* 631:L121
Sakamoto T, Barbier L, Barthelmy SD, Cummings JR, Fenimore EE, et al. 2006. *Ap. J.* 636:L73
Sakamoto T, Lamb DQ, Kawai N, Yoshida A, Graziani C, et al. 2005. *Ap. J.* 629:311
Sako M, Harrison FA, Rutledge RE. 2005. *Ap. J.* 623:973
Salvaterra R, Cerutti A, Chincarini G, Colpi M, Guidorzi C, et al. 2008. *MNRAS* 388:L6
Sari R, Narayan R, Piran T. 1996. *Ap. J.* 473:204
Sari R, Piran T. 1999. *Ap. J.* 517:L109
Sari R, Piran T, Narayan R. 1998. *Ap. J.* 497:L17
Savaglio S, Glazebrook K, LeBorgne D. 2009. *Ap. J.* 691:182
Schaefer BE. 2006. *Ap. J.* 642:L25

Schaefer BE, Gerardy CL, Höflich P, Panaitescu A, Quimby R, et al. 2003. *Ap. J.* 588:387
Setiawan S, Ruffert M, Janka H-T. 2004. *MNRAS* 352:753
Setiawan S, Ruffert M, Janka H-T. 2006. *Astron. Astrophys.* 458:553
Shakura NI, Syunyaev RA. 1973. *Astron. Astrophys.* 24:337
Shaviv NJ, Dar A. 1995. *MNRAS* 277:287
Shibata M, Sekiguchi Y, Takahashi R. 2007. *Prog. Theor. Phys.* 118:257
Shin M-S, Berger E. 2007. *Ap. J.* 660:1146
Soderberg AM, Berger E, Kasliwal M, Frail DA, Price PA, et al. 2006a. *Ap. J.* 650:261
Soderberg AM, Berger E, Page KL, Schady P, Parrent J, et al. 2008. *Nature* 453:469
Soderberg AM, Kulkarni SR, Berger E, Fox DB, Price PA, et al. 2004. *Ap. J.* 606:994
Soderberg AM, Kulkarni SR, Nakar E, Berger E, Cameron PB, et al. 2006b. *Nature* 442:1014
Spada M, Panaitescu A, Mészáros P. 2000. *Ap. J.* 537:824
Spitkovsky A. 2008. *Ap. J.* 673:L39
Spruit HC. 1999. *Astron. Astrophys.* 341:L1
Stanek KZ, Dai X, Prieto JL, An D, Garnavich PM, et al. 2007. *Ap. J.* 654:L21
Stanek KZ, Gnedin OY, Beacom JF, Gould AP, Johnson JA, et al. 2006. *Acta Astronomica* 56:333
Stanek KZ, Matheson T, Garnavich PM, Martini P, Berlind P, et al. 2003. *Ap. J.* 591:L17
Tagliaferri G, Antonelli LA, Chincarini G, Fernandez-Soto A, Malesani D, et al. 2005. *Astron. Astrophys.* 443:L1
Tagliaferri G, Goad M, Chincarini G, Moretti A, Campana S, et al. 2005. *Nature* 436:985
Tanvir NR, Chapman R, Levan AJ, Priddey RS. 2005. *Nature* 438:991
Taylor GB, Frail DA, Berger E, Kulkarni SR. 2004. *Ap. J.* 609:L1
Taylor GB, Momjian E, Pihlström Y, Ghosh T, Salter C. 2005. *Ap. J.* 622:986
Thompson C. 1994. *MNRAS* 270:480
Thompson C. 2006. *Ap. J.* 651:333
Thompson C, Mészáros P, Rees MJ. 2007. *Ap. J.* 666:1012
Thompson TA, Chang P, Quataert E. 2004. *Ap. J.* 611:380
Thompson TA, Quataert E, Burrows A. 2005. *Ap. J.* 620:861
Thöne CC, Fynbo JPU, Östlin G, Milvang-Jensen B, Wiersema K, et al. 2008. *Ap. J.* 676:1151
Tremonti CA, Heckman TM, Kauffmann G, Brinchmann J, Charlot S, et al. 2004. *Ap. J.* 613:898
Tumlinson J, Prochaska JX, Chen H-W, Dessauges-Zavadsky M, Bloom JS. 2007. *Ap. J.* 668:667
Usov VV. 1992. *Nature* 357:472
Uzdensky DA, MacFadyen AI. 2007. *Ap. J.* 669:546
van der Horst AJ, Kamble A, Wijers RAMJ, Resmi L, Bhattacharya D, et al. 2007. *R. Soc. Lond. Philos. Trans. Ser. A* 365:1241
van Paradijs J, Groot PJ, Galama T, Kouveliotou C, Strom RG, et al. 1997. *Nature* 386:686
van Paradijs J, Kouveliotou C, Wijers RAMJ. 2000. *Annu. Rev. Astron. Astrophys.* 38:379
Vestrand WT, Woźniak PR, Wren JA, Fenimore EE, Sakamoto T, et al. 2005. *Nature* 435:178
Vestrand WT, Wren JA, Woźniak PR, Aptekar R, Golentskii S, et al. 2006. *Nature* 442:172
Villasenor JS, Lamb DQ, Ricker GR, Atteia J-L, Kawai N, et al. 2005. *Nature* 437:855
Vreeswijk PM, Ellison SL, Ledoux C, Wijers RAMJ, Fynbo JPU, et al. 2004. *Astron. Astrophys.* 419:927
Vreeswijk PM, Ledoux C, Smette A, Ellison SL, Jaunsen AO, et al. 2007. *Astron. Astrophys.* 468:83
Wainwright C, Berger E, Penprase BE. 2007. *Ap. J.* 657:367
Waxman E. 1995. *Phys. Rev. Lett.* 75:386
Waxman E. 2004a. *Ap. J.* 605:L97
Waxman E. 2004b. *New J. Phys.* 6:140
Waxman E. 2004c. *Ap. J.* 606:988
Waxman E. 2006. *Nucl. Phys. B Proc. Suppl.* 151:46
Waxman E, Bahcall J. 1997. *Phys. Rev. Lett.* 78:2292
Waxman E, Bahcall J. 1999. *Phys. Rev. D* 59(2):023002
Waxman E, Kulkarni SR, Frail DA. 1998. *Ap. J.* 497:288
Waxman E, Mészáros P. 2003. *Ap. J.* 584:390
Waxman E, Mészáros P, Campana S. 2007. *Ap. J.* 667:351

Willingale R, O'Brien PT, Osborne JP, Godet O, Page KL, et al. 2007. *Ap. J.* 662:1093
Woods E, Loeb A. 1995. *Ap. J.* 453:583
Woosley SE. 1993. *Ap. J.* 405:273
Woosley SE, Bloom JS. 2006. *ARAstron. Astrophys.* 44:507
Woźniak PR, Vestrand WT, Panaitescu AD, Wren JA, Davis HR, et al. 2009. *Ap. J.* 691:495
Woźniak PR, Vestrand WT, Wren JA, White RR, Evans SM, et al. 2006. *Ap. J.* 642:L99
Yoshida A, Namiki M, Otani C, Kawai N, Murakami T, et al. 1999. *Astron. Astrophys.S* 138:433
Yost SA, Alatalo K, Rykoff ES, Aharonian F, Akerlof CW, et al. 2006. *Ap. J.* 636:959
Yüksel H, Kistler MD, Beacom JF, Hopkins AM. 2008. *Ap. J.* 683:L5
Zerbi RM, Chincarini G, Ghisellini G, Rondonó M, Tosti G, et al. 2001. *Astronomische Nachrichten* 322:275
Zhang B. 2007. *Chinese J. Astron. Astrophys.* 7:1
Zhang B, Fan YZ, Dyks J, Kobayashi S, Mészáros P, et al. 2006. *Ap. J.* 642:354
Zhang B, Kobayashi S, Mészáros P. 2003. *Ap. J.* 595:950
Zhang W, MacFadyen A, Wang P. 2009. *Ap. J.* 692:L40
Zhang W, Woosley SE, Heger A. 2004. *Ap. J.* 608:365
Zheng Z, Ramirez-Ruiz E. 2007. *Ap. J.* 665:1220
Zou Y-C, Piran T, Sari R. 2009. *Ap. J.* 692:L92

Annual Review of Astronomy and Astrophysics

Volume 47, 2009

Contents

Indexes

Errata

An online log of corrections to *Annual Review of Astronomy and Astrophysics* articles may be found at http://astro.annualreviews.org/errata.shtml